Analysis for the information of neural cell nuclei in the postnatal cerebral cortex using mouse cloning technique

Hatsune Makino

DOCTOR OF PHILOSOPHY

Department of Physiological Sciences

School of Life Science

The Graduate University for Advanced Studies

2003

Contents

Acknowledgements

Chapter 1

Analysis of the developmental totipotency of the nuclei of differentiated neurons of the postnatal mouse cerebral cortex using mouse cloning

Abstract

Successful mouse cloning has been achieved using several types of somatic cell nuclei. However, cloned mice and fetuses have never been obtained using the nuclei of adult neurons from the cerebral cortex. In a previous report, I successfully produced cloned mice using the nuclei of fetal neural cells from the cerebral cortex. To examine the totipotency of neuronal nuclei for normal development, here I attempted to generate cloned mice using the nuclei of NeuN-positive differentiated neurons from the cerebral cortex of postnatal day 0 to 4 mice. I obtained no cloned full-term pups, but cloned fetuses were obtained at 10.5 days postcoitum at a high rate. However, many of these fetuses had morphological abnormalities of the neural tube, including an open anterior neuropore and/or undulation. At the cytoarchitectural level, abnormalities included spherical omission of the neuroepithelium, collapsed neural tube lumen, and markedly abnormal expression patterns of neuronal markers. These results indicated that the nuclei of differentiated neurons are not totipotent and cannot drive normal development. These defects were also found when differentiated cortical plate nuclei from the embryonic cerebral cortex were used. Thus, the nuclei of differentiated neurons in the cerebral cortex may not undergo the reprogramming required to drive the normal development of the early embryonic stages.

Introduction

The brain is a highly organized structure containing an enormous number of neural cells. Diversity in the cerebral cortex occurs not only in the number of neural cells but also in the innumerable combinations of cell-cell interactions. In the mammalian brain, the timing of the appearance of neurons in the developing nervous system is highly reproducible, and neurons are generated primarily during the embryonic period. In the mouse cerebral cortex, neurogenesis begins around 12.5 days postcoitum (dpc), when the multipotent stem cells that generate both neurons and glia are the major components of the early neuroepithelium, peaks around 15.5 dpc, and concludes around birth (Bayer and Altman, 1991). The completely differentiated neurons in the adult cerebral cortex never divide.

When neurons derived from adult mouse cerebral cortex were used for cloning, neither cloned mice nor fetuses were produced (Wakayama et al., 1998; Osada et al., 2002). In addition, some reconstructed oocytes containing the nuclei of Purkinje cells derived from mice older than 8 weeks have an apparently normal karyotype, but the majority do not (Osada et al., 2002). Oocytes reconstructed using nuclei from immature neural cells derived from the embryonic mouse cerebral cortex at 15.5 dpc developed to healthy adults (Yamazaki et al., 2001). On the other hand, embryos that were cloned using the nuclei of postmitotic, differentiated neurons from the 17.5 dpc cerebral cortex usually failed to become normal pups or fetuses (Yamazaki et al., 2001). These results suggest that the status of the differentiation of donor cells affects the efficiency with which cloned mice are generated and that the nuclei of neural cells in advanced stages of differentiation lose their developmental totipotency during neurogenesis. Still, nobody knows exactly what causes such differences in the efficiency with which cloned

mice are produced using neural cells.

To examine further the developmental potential of the nuclei of differentiated neurons, I tried to produce cloned mice using the nuclei of NeuN-positive, differentiated neurons from the postnatal mouse cerebral cortex. This study examines the relationship between the developmental totipotency of neural cell nuclei and neural cell differentiation.

Materials and methods

Nuclear transfer and oocyte activation

The enucleation of oocytes and donor nucleus injection into them were performed using the Honolulu technique (Wakayama et al., 1998). The inner diameter of the enucleation pipettes was around 10 μm at the tip. Oocytes were handled in Hepes-Chatot-Ziomek-Bavister medium (CZB), which contained 81.62 mM NaCl, 4.83 mM KCl, 1.70 mM $CaCl_2 \cdot 2H_2O$, 1.18 mM $MgSO_4 \cdot 7H_2O$, 1.18 mM KH_2PO_4, 0.11 mM EDTA, 5 mM $NaHCO_3$, 31.30 mM sodium lactate, 0.27 mM sodium Pyruvate, 5.55 mM D-glucose, 1 mM L-glutamine, 100 IU/ml sodium penicillin, 0.7 mM streptomycin, 0.1 mg/ml Polyvinyl alcohol, and 20 mM Hepes (Chatot et al., 1989). The inner diameter of the injection pipettes for the differentiated neurons and cumulus cells was ≈6 and ≈7 μm at the tip and contained a polyvinylpyrrolidone (PVP) suspension in Hepes-CZB. After donor nucleus injection, the reconstructed oocytes were kept for 2 hours in Hepes-CZB before activation by a 6-hour treatment with Ca^{2+}-free modified CZB medium (mCZB, which contained 81.62 mM NaCl, 4.83 mM KCl, 1.70 mM $CaCl_2 \cdot 2H_2O$, 1.18 mM $MgSO_4 \cdot 7H_2O$, 1.18 mM KH_2PO_4, 0.11 mM EDTA, 25.12 mM $NaHCO_3$, 31.30 mM sodium lactate, 0.27 mM sodium Pyruvate, 5.55 mM D-glucose, 1 mM L-glutamine, 100 IU/ml sodium penicillin, 0.7 mM streptomycin, and 5 mg/ml bovine serum albumin) containing 10 mM $SrCl_2$ and 5 $\mu g \cdot ml^{-1}$ Cytochalasin B. Sr^{2+} was used to activate the reconstructed oocytes, and Cytochalasin B was applied to retain all the chromosomes of the donor cell, by preventing the loss of chromosomes into the pseudo polar body during oocyte activation. For long-term culture, mCZB , was used.

Preparation of donor cells for cloning

To obtain B6D2F1 fetuses and pups, C57BL/6J females were mated naturally to DBA/2 males. The day the vaginal plug was observed was designated as 0.5 days postcoitum (dpc), and the day the pups were born was designated as postnatal day zero (P0). Neural cells were collected from wild-type B6D2F1 pups at P0 to P4. The telencephalic region was removed from each fetus and put into Dulbecco's Modified Eagle Medium:Nutrient Mixture F-12 (DMEM/F-12) 1:1 Mixture (GIBCO) containing 10 % fetal bovine serum. The cerebral cortex was dissected from the rest of the telencephalon using a sharp razor blade. Two pieces (around 5 mm in length, divided along the anterior-posterior axis) of the dorsolateral cortex were minced in Hepes-CZB medium. After filtering this cell suspension through a cell strainer containing 40-μm holes (FALCON), the neural cells for cloning were prepared by centrifugation for 3 min at 52 X g or 800 rpm at 4°C. The isolation of cumulus cells was performed as previously described (Wakayama et al., 1998).

Characterization of neurons

Cells around 6 μm in diameter in PVP medium were rinsed with Hepes-CZB medium and then PBS. Either these cells or the filtered cell suspension was plated on MAS-coated glass slides for 1 hr. After aspirating the PBS, the cells were fixed with 4% paraformaldehyde in PBS for 10 min at 4 °C followed by fixation with methanol. They were then incubated with primary antibodies: mouse anti-βIII tubulin (1:2000, Promega) as a marker for differentiated neurons, and mouse anti-NeuN (1:100, Chemicon) as a marker for the nuclei of neurons, followed by an Alexa 488-conjugated goat anti-mouse IgG antibody (1:1000, Molecular Probes). After being washed with

PBS, the cells were stained with DAPI (SIGMA, 1:1,000,000), which labels the nuclei of living cells, for 10 min at room temperature, then washed again with PBS. The nuclei of differentiated neurons in the mouse cerebral cortex at P0-P4 are denoted as "DNn."

Embryo transfer

Cloned embryos that developed to the morula or blastocyst stage were transferred into the uterine horn of 2-day pseudopregnant CD-1 surrogate females mated with vasectomized males of the same strain. Cloned embryos that developed to the 2-cell stage were transferred into the oviducts of 0-day pseudopregnant CD-1 surrogate females mated with vasectomized males of the same strain. B6D2F1 fetuses at 10.5 dpc were used as wild-type fetuses. All cloned fetuses were analyzed at 10.5 dpc. Embryos and 10.5-dpc fetuses that were generated from oocytes containing transferred DNn were named DNnt embryos and DNnt fetuses, respectively.

Histochemistry

Fetuses were analyzed with a LEICA MZ APO microscope with LEICA type 307-072 filters after being washed three times with 0.1 M Phosphate Buffer (PB). Once the data were recorded with an OLYMPUS DP50-CU digital camera and electronically processed, the embryos were fixed by immersion in 4 % paraformaldehyde for 1 hr in 0.1 M PB, pH 7.4 at 4°C, for the histological examination. After being photographed, the embryos were cryoprotected in 25 % sucrose in 0.1 M PB overnight at 4 °C, embedded in 50 % O.C.T. compound (Tissue Tek) diluted with 25 % sucrose in 0.1 M PB, and then frozen on dry ice. Ten-micrometer-thick cryosections were cut and affixed to MAS-coated glass slides. The sections were stained with 0.3 % cresyl violet and then

with methyl green solution to detect nuclei. All the stained sections were dehydrated by serial passage through ethyl alcohol before embedding.

Immunohistochemistry

Standard procedures were adopted for the immunostaining of 10-μm-thick cryosections of fetuses on the MAS-coated glass slides. The primary antibodies used were mouse anti-βIII tubulin (1:2000, Promega) and rabbit anti-Ki-67 (1:1000, Novocastra), a marker for proliferating cells. For detection, fluorescent secondary antibodies Alexa 594-conjugated goat anti-mouse IgG antibody (1:1000, Molecular Probes) and Alexa 488-conjugated goat anti-rabbit IgG antibody (1:1000, Molecular Probes) were used. Cryosections were washed three times with PBS, and blocked in Block Ace (DAINIPPON PHARMASEUTICAL CO., LTD) for 1 hr at room temperature, followed by incubation with primary antibodies diluted in 5 % Block Ace, 0.05 % Triton X-100, and 0.1 % sodium azide in PBS for 4 hrs at room temperature. After being washed three times with PBS, the sections were incubated with secondary antibodies diluted in the same dilution buffer for 1 hr at room temperature. After another three washes with PBS, they were stained with DAPI (1:1,000,000, SIGMA) for 10 min at room temperature, then washed again with PBS. The slides were coverslipped using reagents for preventing fluorescence fading. Specimens were analyzed with an OLYMPUS BX51 microscope and the results were recorded with an OLYMPUS DP50-CU digital camera. All images were processed electronically.

Statistical analysis

Data were analyzed by Fisher's exact probability test.

Results

Selection of neurons for cloning

The cell suspension from postnatal mouse cerebral cortex at P0-P4 (see Materials and methods) contained living cells of various sizes (Fig. 1A, both red and yellow arrows), and some of them were positive for NeuN, which labels neuronal nuclei (Fig. 1B, red arrows). Of the cells in the suspension, I collected for cloning only cells that were around 6 μm in diameter in the PVP media: when cells prepared identically were fixed on glass slides and immunostained with anti-NeuN antibodies, all of them were NeuN positive (Fig. 1C, white arrows and Table 1, 100 % of cells tested). This result strongly indicated that the neural cell nuclei used for cloning in this paper were from differentiated neurons (DNn).

Generation of cloned mice and cloned fetuses using the nuclei of neurons

To examine the developmental potential for producing normal cloned mice, I used single DNn from the cerebral cortex of both female and male mice at P0-P4. I obtained no cloned mice from 184 reconstructed oocytes containing transferred DNn (DNnt) (Table 2). However, I successfully produced 2 healthy pups that were cloned with the nucleus of a cumulus cell, from 134 reconstructed oocytes (Table 2, 2.6% of activated oocytes). Because surrogate mothers that had received cloned embryos with DNn often showed a weight loss between 9.5 dpc and 11.5 dpc, I expected that the DNnt mice died as embryos. Therefore, I sought to generate and observe DNnt fetuses at 10.5 dpc to assess the developmental potential of the neuronal nuclei.

Five hundred and ninety-three activated oocytes that were reconstructed with

neuronal nuclei developed into 237 morula/blastocyst-stage embryos (Table 3, 40.0 % of activated oocytes). After transferring 526 DNnt embryos into pseudopregnant mice, 40 DNnt fetuses were obtained (Table 3, 4.4 % of activated oocytes). This cloning success rate resembled the rate I obtained using cumulus cell nuclei (Table 3, 5.7 % of activated oocytes). The principal features of wild-type fetuses at 8.5-9.0 dpc, at 9.5-10.25 dpc, and at 10.25-10.75 dpc are the turning of the body axis, the appearance of forelimb buds, and closure of the neuropore and appearance of hindlimb buds, respectively (Kaufman et al., 2002). In my experiments, wild-type fetuses at 10.5 dpc exhibited these features and displayed a clear heartbeat. Using these properties of wild-type fetuses as criteria, I defined normal fetuses as having a heartbeat, normal closing of the neural tube, turning of the body axis, and existence of both forelimb buds and hindlimb buds. I obtained 2 normal DNnt (Figs. 2A and 2D, Table 3, 0.2 % of activated oocytes) and 3 normal cumulus-cell-cloned fetuses (Figs. 2J, Table 3, 3.4 % of activated oocytes). The proportion of normal fetuses produced was statistically different between the DNnt fetuses and cumulus-cell fetuses (Table 3, $P < 0.005$). The rate for producing normal DNnt fetuses was similar to the rate I observed previously using fetal post-mitotic differentiated neural cell nuclei (Yamazaki et al., 2001). Thus, my results demonstrated that the nuclei of differentiated neurons maintained the developmental potential to generate DNnt fetuses, although many of the fetuses showed abnormal development.

Morphological characteristics of DNnt fetuses

To further examine the abnormal development of the cloned fetuses, I assessed the morphological features of abnormal fetuses from 38 fetuses cloned from DNnt and 2

from cumulus-cell nuclei. I characterized the cloned fetuses by determining whether or not they showed the 4 criteria described above. Twenty-eight DNnt fetuses did not display a heartbeat (Table 4, 76.3 % of abnormal DNnt fetuses). Thirty-one DNnt fetuses did not show closed neural tubes (Table 4, 81.6 % of abnormal DNnt fetuses). Six DNnt fetuses stopped developing before 8.5 dpc (Table 4, 15.8 % of abnormal DNnt fetuses). Thirty-eight DNnt fetuses showed less-than-normal growth of both the forelimb and hindlimb buds (Table 4, 100 % of abnormal DNnt fetuses). As a result of this classification, I concluded that 38 of the DNnt fetuses (95.0 % of total DNnt fetuses) were abnormal (Figs. 2B, 2C, 2E-2I). Of the cumulus-cell-cloned abnormal fetuses observed, one did not display a heartbeat, closed neural tubes, or turning (Table 4, 50.0 % of cumulus-cell-cloned abnormal fetuses). Two cumulus-cell-cloned abnormal fetuses exhibited less-than-normal growth of both the forelimb and hindlimb buds (Table 4, 100 % of cumulus cell-cloned abnormal fetuses). As a result of this classification, I concluded that the 2 fetuses cloned with cumulus cell nuclei were abnormal (Figs. 2K and 40.0 % of total cumulus-cell-cloned fetuses). The number of fetuses that did not show a closed neural tube and both forelimb and hindlimb buds of the total fetuses was statistically different between DNnt and cumulus-cell-cloned abnormal fetuses (Table 4, $P < 0.05$ and $P < 0.005$, respectively). Moreover, both the DNnt and cumulus-cell-cloned fetuses displayed a distended pericardium (Figs. 2B, 2C, 2G, 2H and 2K, arrows), and excessive blood in the brain, face, heart, and tail (Figs. 2A, 2C, 2F and 2K, arrowheads). Thus, distinct defects were observed in both the DNnt and cumulus-cell-cloned abnormal fetuses. The crown-rump length (CRL), a standard developmental measurement of fetuses, was used to evaluate the feasibility of embryonic staging; this measurement was recorded using a graduated ruler. Compared

to wild-type B6D2F1 fetuses (Fig 2L, 4.33 ± 0.34 mm) (n = 17), DNnt (Figs. 2B, 2C, 2F-2I and Table 4, 2.42 ± 0.71 mm) and cumulus-cell-cloned fetuses (Figs. 2K and Table 3, 1.60 mm) displayed an apparently small body size. These CRL of DNnt fetuses at 10.5 dpc were similar to that of wild-type B6D2F1 fetuses at 9.5 dpc (2.38 ± 0.38 mm) (n = 5) (my preliminary data).

I also compared the morphological features of the abnormal DNnt fetuses with those of the cumulus-cell-cloned abnormal fetuses to better understand the developmental potency of the DNn. The abnormal DNnt fetuses frequently showed a small head (Figs. 2B and 2G), incomplete rotation of the body axis (Figs. 2B, 2G and 2I), persistent opening of the anterior neuropore (Fig. 2B), undulated neural tube closure (Figs. 2B, 2C and 2G-2I), and asymmetrically sized somite pairs (Figs. 2B, 2C and 2G-2I), compared with wild-type littermates. The neural tube defects in the DNnt fetuses and other abnormalities became more severe as the age of the donor mice increased (Table 4). These defects were rarely detected in the cumulus-cell-cloned fetuses. These results indicated that DNn induced unique morphological disorders in the DNnt fetuses with a high frequency.

Abnormalities of the neural tube of DNnt fetuses

To elucidate the disorders of the neural tube in the DNnt fetuses, they were subjected to histological analysis using Nissl staining and immunohistochemical analysis. DNnt fetuses that exhibited an open anterior neuropore and undulated neural tube closure (Figs. 2B, 3A and 3D, arrowheads) or discontinuous neural tube closure (Figs. 2H and 3C) had a thinner neuroepithelium than wild-type fetuses (data not shown). In addition, the former abnormality produced a widespread lack of cells (Fig. 3D) and the latter

displayed neuroepithelium of an uneven thickness (Fig. 3F, arrows) and the disorganization of the ventricular neural cells (Fig. 3F, arrowheads). Even DNnt fetuses that did not show obvious visible defects of the neural tube formed irregular densities of neural cells (Fig. 3E), and small spherical omissions of neural tissue (Fig. 3E, asterisks); these were constructed of erratic cells that had a different polarity from that of the surrounding cells (Fig. 3E, arrows). Disorganization of the ventricular neural cells were observed not only in the neural tube but also in the neuroepithelium of the telencephalon and mesencephalon regions in the DNnt fetuses (data not shown). Also, many pyknotic cells were found in the severely retarded DNnt fetuses by Feulgen staining (data not shown).

Characterizations of the neural tube defects of DNnt fetuses

To further elucidate the abnormalities of the neural tissues in the DNnt (Figs. 2C, 4A and 4B) compared with wild-type (Figs. 2L, 4D and 4E) fetuses, I performed an immunohistological analysis of the neural tubes of DNnt fetuses with anti-βIII tubulin and anti-Ki-67 antibodies to detect neurons and proliferating cells, respectively. DNnt fetuses showing an irregular and distorted closure of the neural tube had organized neuroepithelium that was much thinner (Fig. 4C, arrows) than that of wild-type fetuses (Fig. 4F, arrows). They showed fewer βIII tubulin-positive and Ki-67-positive cells (Fig. 4C) compared with wild-type fetuses (Fig. 4F). Moreover, Nestin-positive neural progenitor cells were scarce in the DNnt fetuses (data not shown). DNnt fetuses exhibited ectopic βIII tubulin expression in the tissues proximal to the neural tube, and the entry points of the motor neurons were unclear (Fig. 4C) compared with wild-type (Fig. 4F, arrowheads). In addition, no proliferating cells were observed at the lumen of

the neural tube (Fig. 4C). Both DNnt fetuses (Fig. 4C) and wild-type fetuses (Fig. 4F) were stained with DAPI (data not shown). Taken together, these results showed that DNnt fetuses with neural tissue abnormalities had irregular localization of neurons and proliferating cells.

My present results can be summarized as follows. DNn derived from the mouse cerebral cortex at P0-P4 lacked developmental potency and could not produce DNnt pups. Abnormalities of DNnt fetuses were frequently observed in the neural tissues. Moreover, the abnormalities were more severe when older donor mice were used. DNnt fetuses had neural tubes that were disorganized at the cytoarchitectural level and constructed with an irregular distribution of neurons and proliferating cells.

Discussion

Developmental potency of embryos cloned using neural cell nuclei

The cloning success rate (the proportion of morulae/blastocysts that developed from all the activated oocytes, i.e., those forming 2-cell-stage embryos) using DNn (Table 2, 40.0 %,) was higher than the rate obtained using medulloblastoma cells originating from granule neuron precursors in the developing cerebellum (13.1%) (Li et al., 2003), mature olfactory sensory neurons (13.6 %) (Eggan et al., 2004), E14 ES cells (21.8 %) (Wakayama et al., 1999a), cumulus cells (36.2 %) (data not shown), or fetal neural cells (36.6 %) (Yamazaki et al., 2001). The rate was similar to that obtained using Sertoli cells (39.6 %) (Wakayama et al., 1998) and was lower than the rate obtained using male germ cells at 12.5-15.5 dpc (54-100 %) (Yamazaki et al., 2003). The percentage of normal fetuses developing from 2-cell-stage embryos when DNn was used for the cloning (Table 2, 0.2 %) was lower than the rate obtained using neural cell nuclei from mouse embryos at 15.5 dpc (10.3 %), premature or early-differentiated neural cell nuclei from mouse embryos at 17.5 dpc (5.9 %), or nuclei of postmitotic-differentiated neurons from mouse embryos at 17.5 dpc (0.3 %) (Yamazaki et al., 2001). Taking these results together with the fact that embryos cloned with the nuclei of fully differentiated neurons have never developed into normal pups, my findings and previous reports suggest that the nuclei of neural cells lose their developmental totipotency as they differentiate.

Components of the early postnatal mouse cerebral cortex

Using immunostaining with NeuN, I have shown that my method for obtaining

neurons is successful, and I used the nuclei of cells obtained with the same method to produce DNnt fetuses (Table 1); I was not, however, able to confirm that the specific cells used to generate the DNnt fetuses were NeuN-positive, because they could not be used as donor cells for cloning after the immunohistochemical treatment. Cells composing the mouse cerebral cortex have been classified by immunostaining with the following marker antibodies: Nestin (for neural progenitor cells), βIII tubulin (for neurons), O4 (for immature oligodendrocytes), and GFAP (for astrocytes), and their ratios in normal mice have been calculated (Qian et al., 2000). At P0, Nestin-, βIII tubulin-, O4-, and GFAP-positive cells are observed as 6.48 %, 50.35 %, 0.22 %, and 1.58 % of the cerebral cortex cells, respectively, and at P3-P4, 22.01 %, 59.34 %, 0.55 %, and 4.58 %, respectively (Qian et al., 2000). When I stained cell suspensions from the P0, P1, and P2 mouse cerebral cortex with βIII-tubulin antibodies, 48.9 % (204/417), 53.3 % (203/381), and 57.5 % (233/405) of these cells were neurons; i.e., their nuclei were positive for both βIII-tubulin and DAPI (my preliminary data). NeuN is a DNA-binding, neuron-specific protein that is expressed in most vertebrate neuronal cell types. Because previous reports have confirmed that NeuN-positive cells are neurons (Wolf et al., 1996), here I assumed these cells to be differentiated neurons and used their nuclei for mouse cloning.

Relationship between cell differentiation and the cloning success rate

When using neural cells from the entire cerebral cortex of mouse embryos at 15.5 dpc for cloning, both normal fetuses and normal full-term pups were generated at a high frequency (Yamazaki et al., 2001). Using the nuclei of premature and early-differentiated neural cells for nuclear transfer, both normal fetuses and fertile

full-term pups were produced (Yamazaki et al., 2001). In contrast, almost no morphologically normal fetuses and healthy full-term pups were obtained when postmitotic-differentiated neurons from the subpial cortex were used for cloning (Yamazaki et al., 2001). In this study, some fetuses cloned using the nuclei of NeuN-positive cells derived from postnatal mouse cerebral cortex were generated. However, no full-term pups were obtained. The fetuses displayed morphological abnormalities similar to those of fetuses cloned using the nuclei of postmitotic-differentiated neurons (Yamazaki et al., 2001). When the nuclei of neural cells derived from adult mouse cerebral cortex were used for the nuclear transfer, neither fetuses nor full-term pups were obtained (Wakayama et al., 1998; Osada et al., 2002). Thus, the nuclei of NeuN-positive neurons had a potential similar to that of postmitotic-differentiated neurons.

The success rate for producing cloned fetuses and pups tended to decrease when nuclei from neurons of an older mouse cortex were used. This finding also supports the hypothesis that the nuclei of neural cells lose their totipotency for embryogenesis and neurogenesis during neural cell differentiation. When embryos cloned using adult fully differentiated neurons show evidence of chromosomal disorders, their development stops at the 2-cell stage (Osada et al., 2002), suggesting that DNnt embryos and DNnt fetuses must contain very few chromosomal abnormalities. No notable morphological defects of the neural tissues of DNnt fetuses were recognized when cumulus cell nuclei (Figs. 2J and 2K and Table 4) and fibroblast cell nuclei (data not shown) were used for generating cloned mice. These abnormalities have only been reported when nuclei from cells of the subpial cortex of fetal mice were used (Yamazaki et al., 2001). These results indicate that the efficiency of the production of healthy cloned mice and normal cloned

fetuses is dependent on the differentiation level of the donor cells, and moreover, that the neural tissue disorders seen in some of these cloned mice represent a distinctive phenotype that is induced by failures in the reprogramming of the DNn.

Distinctive features of fetuses cloned using neural cell nuclei

Developmental retardation, including a small head, incomplete rotation of the body axis, open anterior neuropore, undulated neural tube closure, and asymmetrically sized somite pairs, were common in the DNnt fetuses. Most of them died by 10.5 dpc, and showed neural tube abnormalities including an unusual lack of neuroepithelial cells, few proliferating cells, and abnormal expression patterns of a neural cell marker. About half of the fetuses cloned using cumulus cell nuclei also displayed developmental delay at 10.5 dpc including a distended pericardium and excessive blood. However, the abnormal phenotypes of the neural tubes were seen significantly more often when the nuclei of differentiated neurons were used. These findings indicate that the nuclei of differentiated neurons might possess a common property that causes them to induce neural abnormalities in the cloned fetuses. It is possible that the nuclei of differentiated neurons can only rarely undergo reprogramming after being injected into the oocyte.

A small head, incomplete rotation of the body axis, open anterior neuropore, undulated neural tube closure, distended pericardial cavity, and irregular somitogenesis are regulated by *Notch1,* which has a general role as a segmentation clock (Conlon et al., 1995; Jiang et al., 2000). These abnormalities, which I observed in the DNnt fetuses, have also been identified in the knockout fetuses of *Notch1* (Swiatek et al., 1994), the mammalian homologue 1 of *Drosophila Enhancer of split* (*HES1*) (Ishibashi et al., 1995), recombination signal-binding protein-Jκ (*RBP-Jκ*) (Oka et al., 1995), and

N-cadherin (Radice et al., 1995; Luo et al., 2001). These molecules play critical roles in maintaining the balance between cell proliferation, differentiation, and apoptosis in early neurogenesis.

The curious spherical omissions of neuroepithelial tissue in the DNnt fetuses (Fig. 3E) are similar to rosette-like structures observed in *HES1* (Kageyama et al., 1997; Tomita et al., 1996) and *N-cadherin* (Kostetskii et al., 2001) null mutants. Rosette-like structures are constructed with postmitotic immature neurons in *HES1*-knockout fetuses, in which there is no inhibition of *Mash1* gene expression by *HES1*, and similar structures containing ependymal lining in their centers are seen in N-cadherin null fetuses (Kostetskii et al., 2001). The composition of the rosette-like structures in the DNnt fetuses has not yet been elucidated.

Although further studies are required to elucidate the mechanisms of the neural tube malformations in the DNnt fetuses, my findings suggest that nuclei of the differentiated neurons from the cerebral cortex did not have sufficient differentiation potency to undergo normal early neurogenesis.

Genes required for normal embryogenesis in the cloned mouse fetuses

In addition to the abnormalities described above, a severely enlarged pericardial cavity in the fetuses cloned using the nuclei of DN (Figs. 2B, 2C, 2G and 2H), cumulus cells (Fig. 2K), and neural cells at 15.5-17.5 dpc (Yamazaki et al., 2001) has also been detected in *Notch1* and *RBP-Jκ* null mutants, and the latter exhibit abnormal placental development (Oka et al., 1995). *Notch1*-, *RBP-Jκ*–, and *N-cadherin*-null mutants show embryonic lethality before 11.5 dpc (Swiatek et al., 1994), 10.5 dpc (Oka et al., 1995), and 10.5 dpc (Radice et al., 1997), respectively, like the DNnt fetuses (Table 2).

Considering these reports, and the facts that *Notch1*-null mutants carry extensive defects in angiogenic vascular remodeling that affect the placenta (Krebs et al., 2000), and that *Notch1*-mediated activation of *HES1* inhibits the expression of *Mash1* (Chen et al., 1997), which is required for differentiation of the pulmonary neuroendocrine cells (Ito et al., 2000), an incomplete Notch signaling cascade may contribute not only to the ballooning pericardial cavity in the cloned fetuses, including the DNnt fetuses, but also to the abnormal symptoms of pulmonary hypertension and placental overgrowth in the cloned animals (Wakayama et al., 1999b; Lanza et al., 2000; Tamashiro et al., 2000). My results suggest that defective somitogenesis may depend on the Notch signaling cascades.

Roles of genomic information in donor nuclei in the cloned embryos

In this study, I obtained blastocysts at high frequency that were cloned using DNn and cumulus cell nuclei (Table 2). If I compare this finding with the results obtained using adult neurons (Osada et al., 2002), it appears that DNn derived from the postnatal mouse cerebral cortex could easily be reprogrammed in early embryogenesis, whereas neurons in the adult mouse cerebral cortex could not. Both this difference in cloning success rates (Table 2) and the unevenness of the expression patterns of imprinted genes in the clone-derived placentas at term (Inoue et al., 2002) may depend on the donor cell nuclei, and they may involve regulation by mechanisms besides the common epigenetic alteration systems (Rideout et al., 2001). DNnt fetuses showed morphological abnormalities in their neural tissues that were similar to those of fetuses cloned using postmitotic-differentiated neurons from the pial side of the fetal cerebral cortex (Yamazaki et al., 2001), and they never reached term. Thus, my findings confirmed

previous results, and supported my assertion that the nuclei of differentiated neurons are reprogrammed insufficiently to generate normal embryos.

When using the nuclei of terminally differentiated B and T lymphocytes to generate cloned mice, neither cloned mice nor fetuses were produced (Hochedlinger and Jaenisch, 2002), as when adult neurons were used for cloning. In contrast, healthy mice were generated from ES cells that were derived from blastocysts that were cloned using the nuclei of mature, differentiated B and T lymphocytes (Hochedlinger and Jaenisch, 2002). In addition, recent studies demonstrated that healthy mice could be generated from ES cells derived from blastocysts that were cloned with the nuclei of mature olfactory sensory neurons, using the tetraploid blastocyst injection technique (Eggan et al., 2004). These reports suggest that ES cells are reprogrammed completely during embryogenesis. No one knows why ES cells can be easily reprogrammed while adult differentiated cells cannot. However, these previous reports and my data in this paper provide good evidence that I may be able to obtain healthy mice that are constructed with ES cells derived from blastocysts cloned using DNn. I will have to establish ES cell lines from blastocysts cloned using the nuclei of neurons to understand the developmental potencies of single differentiated neurons, by assessing the genomic information carried by the ES cells.

References

Bayer, S. A., Altman, J., 1991. Development of the endopiriform nucleus and the claustrum in the rat brain. Neuroscience 45, 391-412.

Chatot, C. L., Ziomek, C. A., Bavister, B. D., Lewis, J. L., Torres, I., 1989. An improved culture medium supports development of random-bred 1-cell mouse embryos in vitro. J. Reprod. Fertil. 86, 679-688.

Chen, H., Thiagalingam, A., Chopra. H., Borges, M. W., Feder, J. N., Nelkin, B. D., Baylin, S. B., Ball, D. W., 1997. Conservation of the Drosophila lateral inhibition pathway in human lung cancer: a hairy-related protein (HES-1) directly represses achaete-scute homolog-1 expression. Proc. Natl. Acad. Sci. USA 94, 5355-5360.

Conlon, R. A., Reaume, A. G., Rossant, J., 1995. Notch1 is required for the coordinate segmentation of somites. Development 121, 1533-1545.

Eggan, K., Baldwin, K., Tackett, M., Osborne, J., Gogos, J., Chess, A., Axel, R., Jaenisch R., 2004. Mice cloned from olfactory sensory neurons. Nature 428, 44-49.

Hochedlinger, K., Jaenisch, R., 2002. Monoclonal mice generated by nuclear transfer from mature B and T donor cells. Nature 415, 1035-1038.

Inoue, K., Kohda, T., Lee, J., Ogonuki, N., Mochida, K., Noguchi, Y., Tanemura, K.,

Kaneko-Ishino, T., Ishino, F., Ogura, A., 2002. Faithful expression of imprinted genes in cloned mice. Science 295, 297.

Ishibashi, M., Ang, S. L., Shiota, K., Nakanishi, S., Kageyama, R., Guillemot, F., 1995. Targeted disruption of mammalian hairy and Enhancer of split homolog-1 (HES-1) leads to up-regulation of neural helix-loop-helix factors, premature neurogenesis, and severe neural tube defects. Genes Dev. 9, 3136-3148.

Ito, T., Udaka, N., Yazawa, T., Okudela, K., Hayashi, H., Sudo, T., Guillemot, F., Kageyama, R., Kitamura, H., 2000. Basic helix-loop-helix transcription factors regulate the neuroendocrine differentiation of fetal mouse pulmonary epithelium. Development 127, 3913-3921.

Jiang, Y. J., Aerne, B. L., Smithers, L., Haddon, C., Ish-Horowicz, D., Lewis, J., 2000. Notch signalling and the synchronization of the somite segmentation clock. Nature 408, 475-479.

Kageyama, R., Ishibashi, M., Takebayashi, K., Tomita, K., 1997. bHLH transcription factors and mammalian neuronal differentiation. Int. J. Biochem. Cell Biol. 29, 1389-1399.

Kaufman, H. M., 2002. The atlas of mouse development (Fifth printing of revised edition).

Kostetskii, I., Moore, R., Kemler, R., Radice, G. L., 2001. Differential adhesion leads to segregation and exclusion of N-cadherin-deficient cells in chimeric embryos. Dev. Biol. 234, 72-79.

Krebs, L. T., Xue, Y., Norton, C. R., Shutter, J. R., Maguire, M., Sundberg, J. P., Gallahan, D., Closson, V., Kitajewski, J., Callahan, R., Smith, G. H., Stark, K. L., Gridley, T., 2000. Notch signaling is essential for vascular morphogenesis in mice. Genes Dev. 14, 1343-1352.

Lanza, R. P., Cibelli, J. B., Blackwell, C., Cristofalo, V. J., Francis, M. K., Baerlocher, G. M., Mak, J., Schertzer, M., Chavez, E. A., Sawyer, N., Lansdorp, P. M., West, M. D., 2000. Extension of cell life-span and telomere length in animals cloned from senescent somatic cells. Science 288, 665-669.

Li, L., Connelly, M. C., Wetmore, C., Curran, T., Morgan, J. I., 2003. Mouse embryos cloned from brain tumors. Cancer Res. 63, 2733-2736.

Luo, Y., Ferreira-Cornwell, M., Baldwin, H., Kostetskii, I., Lenox, J., Lieberman, M., Radice, G., 2001. Rescuing the N-cadherin knockout by cardiac-specific expression of N- or E-cadherin. Development 128, 459-469.

Oka, C., Nakano, T., Wakeham, A., de la Pompa, J. L., Mori. C., Sakai, T., Okazaki, S., Kawaichi, M., Shiota, K., Mak, T. W., Honjo, T., 1995. Disruption of the mouse RBP-Jκ gene results in early embryonic death. Development 121, 3291-3301.

Osada, T., Kusakabe, H., Akutsu, H., Yagi, T., Yanagimachi, Y., 2002. Adult murine neurons: their chromatin and chromosome changes and failure to support embryonic development as revealed by nuclear transfer. Cytogenet. Genome Res. 97, 7-12.

Qian, X, Shen, Q., Goderie, S. K., He, W., Capela, A., Davis, A. A., Temple, S., 2000. Timing of CNS cell generation: A programmed sequence of neuron and glial cell production from isolated murine cortical stem cells. Neuron 28, 69-80.

Radice, G. L., Rayburn, H., Matsunami, H., Knudsen, K. A., Takeichi, M., Hynes, R. O., 1997. Developmental defects in mouse embryos lacking N-cadherin. Dev. Biol. 181, 64-78.

Rideout, W. M 3rd., Eggan, K., Jaenisch, R., 2001. Nuclear cloning and epigenetic reprogramming of the genome. Science 293, 1093-1098.

Swiatek, P. J., Lindsell, C. E., del Amo, F. F., Weinmaster, G., Gridley, T., 1994. Notch1 is essential for postimplantation development in mice. Genes Dev. 8, 707-719.

Tamashiro, K. L., Wakayama, T., Blanchard, R. J., Blanchard, D. C., Yanagimachi, R., 2000. Postnatal growth and behavioral development of mice cloned from adult cumulus cells. Biol. Reprod. 63, 328-334.

Tomita, K., Ishibashi, M., Nakahara, K., Ang, S. L., Nakanishi, S., Guillemot, F.,

Kageyama, R., 1996. Mammalian hairy and Enhancer of split homolog 1 regulates differentiation of retinal neurons and is essential for eye morphogenesis. Neuron 16, 723-734.

Wakayama, T., Perry, A. C. F., Zuccoti, M., Johnson, K. R., Yanagimachi, R., 1998. Full-term development of mice from enucleated oocytes injected with cumulus cell nuclei. Nature 394, 369-374.

Wakayama, T., Rodriguez, I., Perry, A. C., Yanagimachi, R., Mombaerts, P., 1999a. Mice cloned from embryonic stem cells. Proc. Natl. Acad. Sci. USA 96, 14984-14989.

Wakayama, T., Yanagimachi, R., 1999b. Cloning of male mice from adult tail-tip cells. Nat. Genet. 22, 127-128.

Wolf, H. K., Buslei, R., Schmidt-Kastner, R., Schmidt-Kastner, P. K., Pietsch, T., Wiestler, O. D., Bluhmke, I., 1996. NeuN: a useful neuronal marker for diagnostic histopathology. J. Histochem. Cytochem. 44, 1167-1171.

Yamazaki, Y., Makino, H., Hamada-Hamaguchi, K., Hamada, S., Sugino, H., Kawase, E., Miyata, T., Ogawa, M., Yanagimachi, R., Yagi, T., 2001. Assessment of the developmental totipotency of neural cells in the cerebral cortex of mouse embryo by nuclear transfer. Proc. Natl. Acad. Sci. USA 98, 14022-14026.

Yamazaki, Y., Mann, M.R., Lee, S. S., Marh, J., McCarrey, J. R., Yanagimachi R., Bartolomei, M. S., 2003. Reprogramming of primordial germ cells begins before migration into the genital ridge, making these cells inadequate donors for reproductive cloning. Proc. Natl. Acad. Sci. USA 100, 12207-12212.

Fig. 1. Characterization of differentiated neurons.

Immunostaining of the cell mixtures derived from the P0-P4 mouse cerebral cortex in Hepes-CZB media (A and B) with DAPI (blue) for the detection of living cell nuclei (A) and anti-NeuN antibodies as a differentiated neural cell marker (black) (B). Red arrows indicate cells that were positive for both DAPI and NeuN, which were differentiated neurons and 6 to 7 μm in diameter (A and B). Yellow arrows indicate DAPI-positive and NeuN-negative cells (A and B). Differentiated neural cells 6 to 7 μm in diameter shrank in the PVP solution used in the cell suspensions for nuclear transfer; therefore, these cells were around 6 μm in diameter (white arrow in C). (Scale bars, 10 μm.)

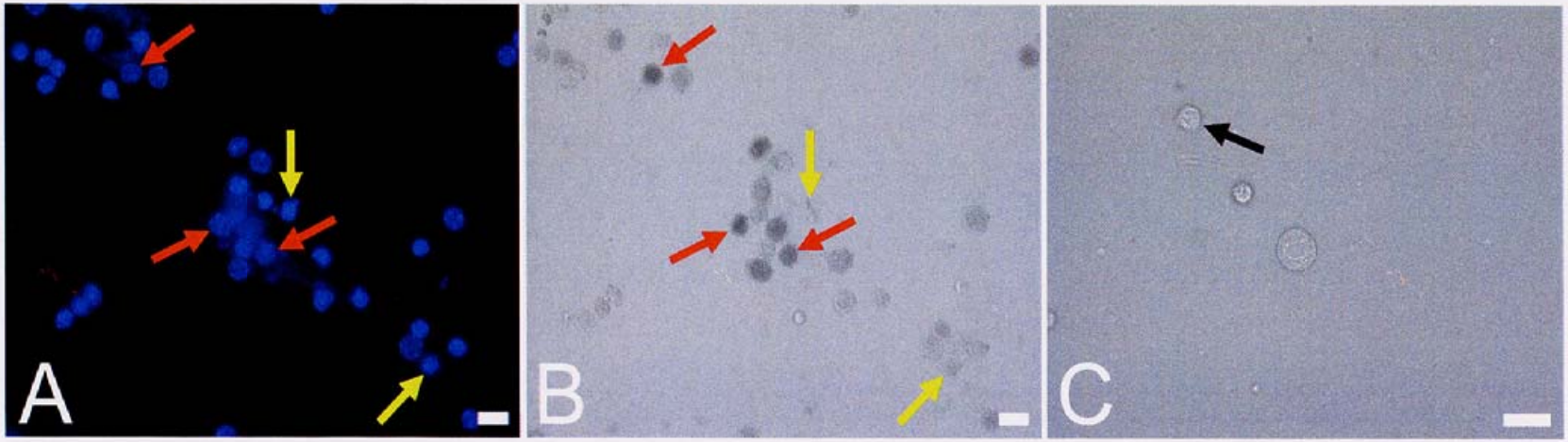

Figure. 1

Fig. 2. Fetuses at 10.5 dpc cloned using the nuclei of neurons (DNnt fetuses).

Fetuses were cloned using the nuclei of neurons from the mouse cerebral cortex at P0 (A and B), P1 (C and D), P2 (E and F), P3 (G), and P4 (H and I), and using cumulus cell nuclei (J and K). A wild-type B6D2F1 fetus is shown in L. Normal fetuses are shown in A, D, J and L. The majority of DNnt fetuses showed abnormalities, including a small head (B and G), incomplete rotation of the body axis (B, G, and I), opening of the anterior neuropore (B), continuous undulated closure of the neural tube (B, C, and G-I), and asymmetrically sized somite pairs (B, C, and G-I). The cloned fetuses displayed retardation (B, C, E-I, and K), distended pericardium (arrows in B, C, G, H and K), and abnormal blood flow (Small double arrowheads in A, C, F, and K). (Scale bar, 1 mm; is applied to all fetuses in this figure.)

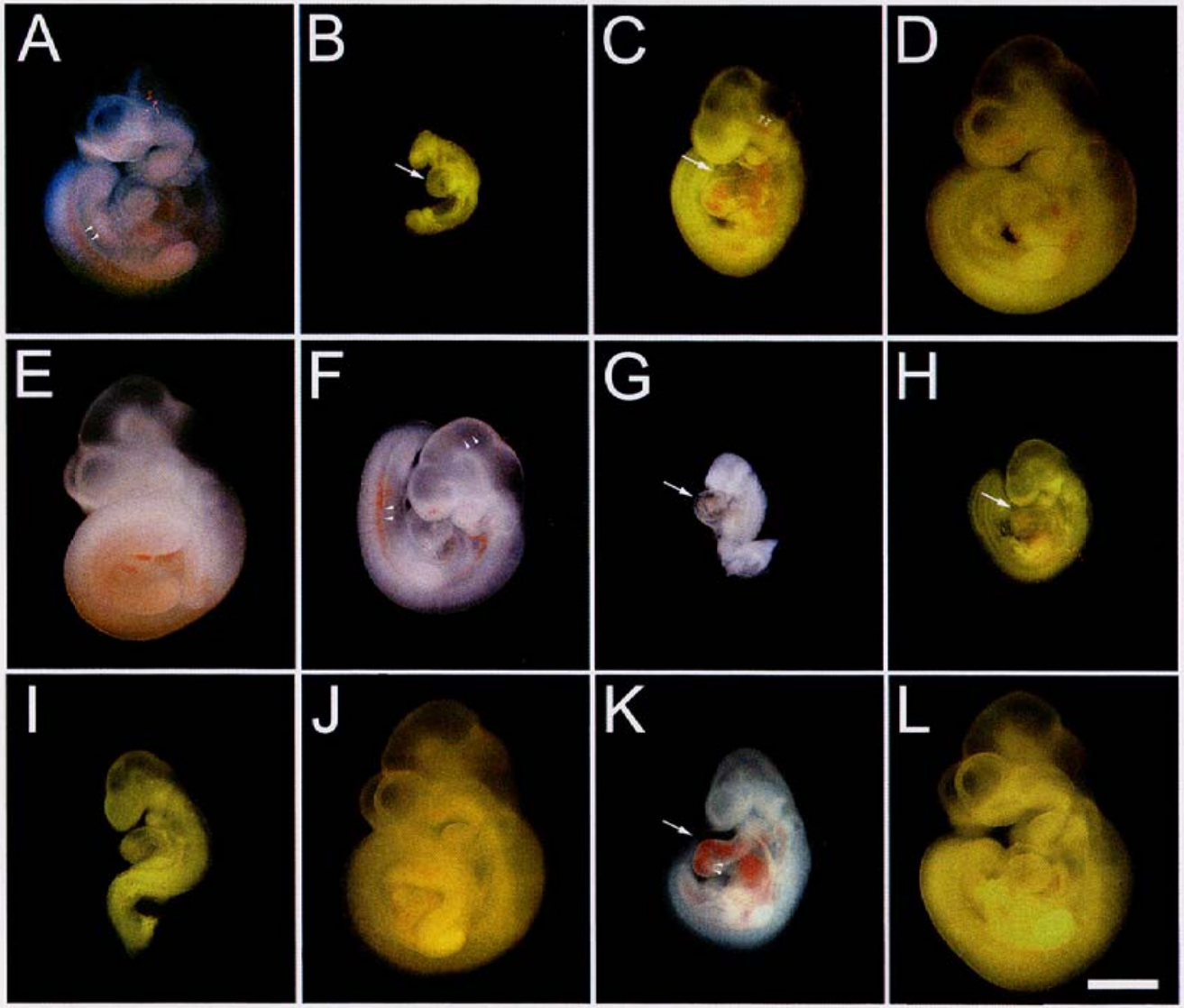

Figure. 2

Fig. 3. Morphological defects of the neural tube of DNnt fetuses.

Fetuses cloned using DNn in the mouse cerebral cortex at P0 (A and D), P1 (B and E), and P4 (C and F) were Nissl-stained after transverse sectioning (D, E, and F). DNnt fetuses showed not only gross defects including an anterior neuropore (large arrowheads in A), undulatory neural tube (small arrowheads in A), and interrupted neural tube closure (arrowheads in C), but also a disorganized neuroepithelium, including an abnormal loss of cells (D), irregular density of neural cells (E), spherical omission of neuroepithelium (asterisks in E), uneven thickness of neuroepithelium (pair of arrows in F), and collapse of the ventricular zone organization (arrowheads in F). (Scale bars in A, D, E, and F, 100 μm; in B and C, 0.5 mm.)

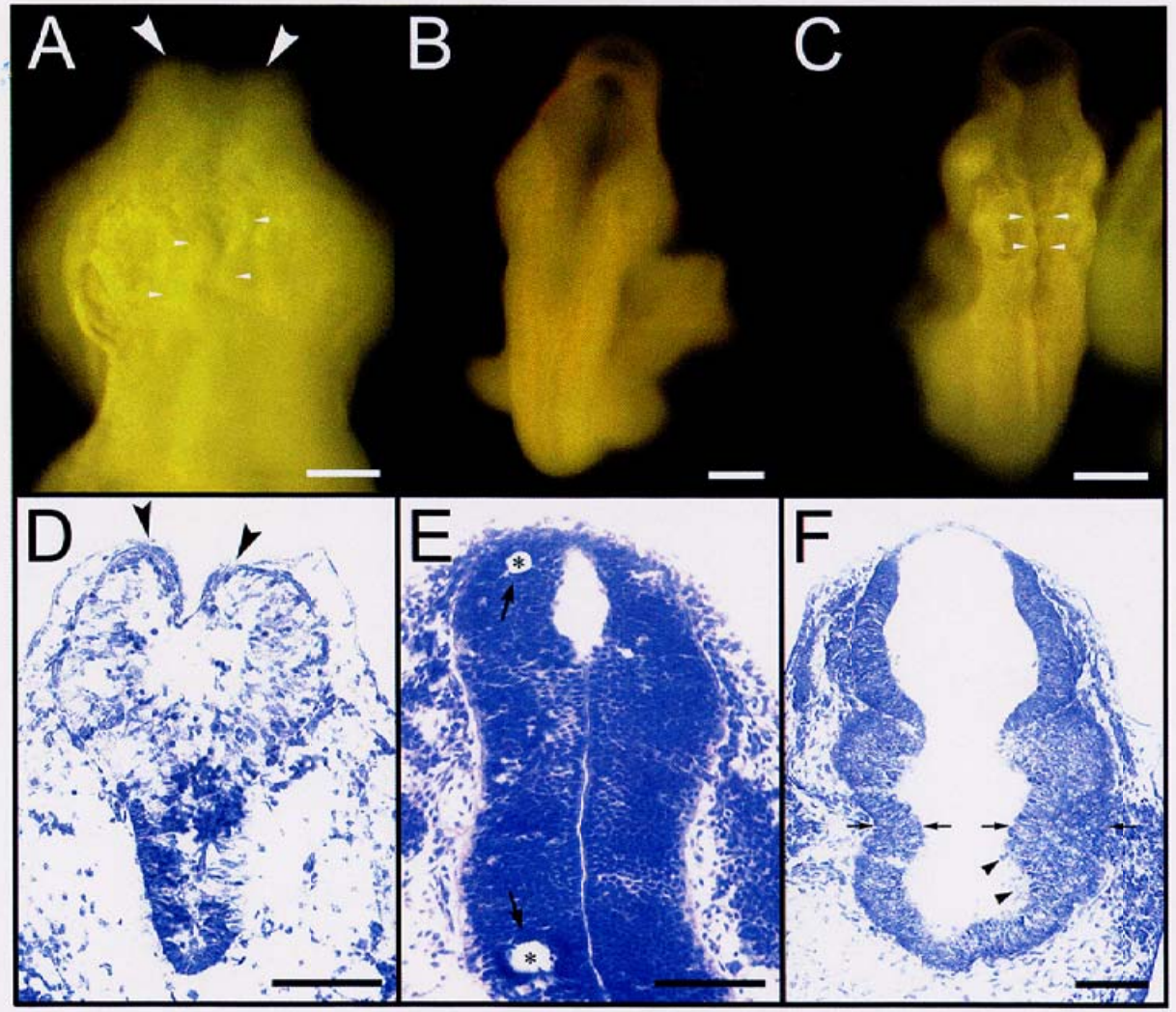

Figure. 3

Fig. 4. Expression patterns of a neuron-specific marker in the neural tube of DNnt fetuses.

Transverse sections of a fetus cloned using DNn from the mouse cerebral cortex at P1 showing severe distortion of the neural tube closure (B) with a neuroepithelium that was much thinner than that of wild-type mice (pair of arrows in C and F), and with systemic congestion (A), and sections from a wild-type fetus (D and E) were immunostained with both anti-βIII tubulin antibodies (red) as a marker for neurons and anti-Ki-67 antibodies (bright green) to detect proliferating cells (C and F). DNnt fetuses showed ectopic βIII tubulin expression in the tissues proximal to the neural tube, and unclear entry points of motor neurons (C), as compared with the wild-type fetus (arrowheads in F), and there were no proliferating cells at the ventricular zone of the neural tube (C). (Scale bars in A and D, 0.5 mm; in B and E, 100 μm; in C and E, 50 μm.)

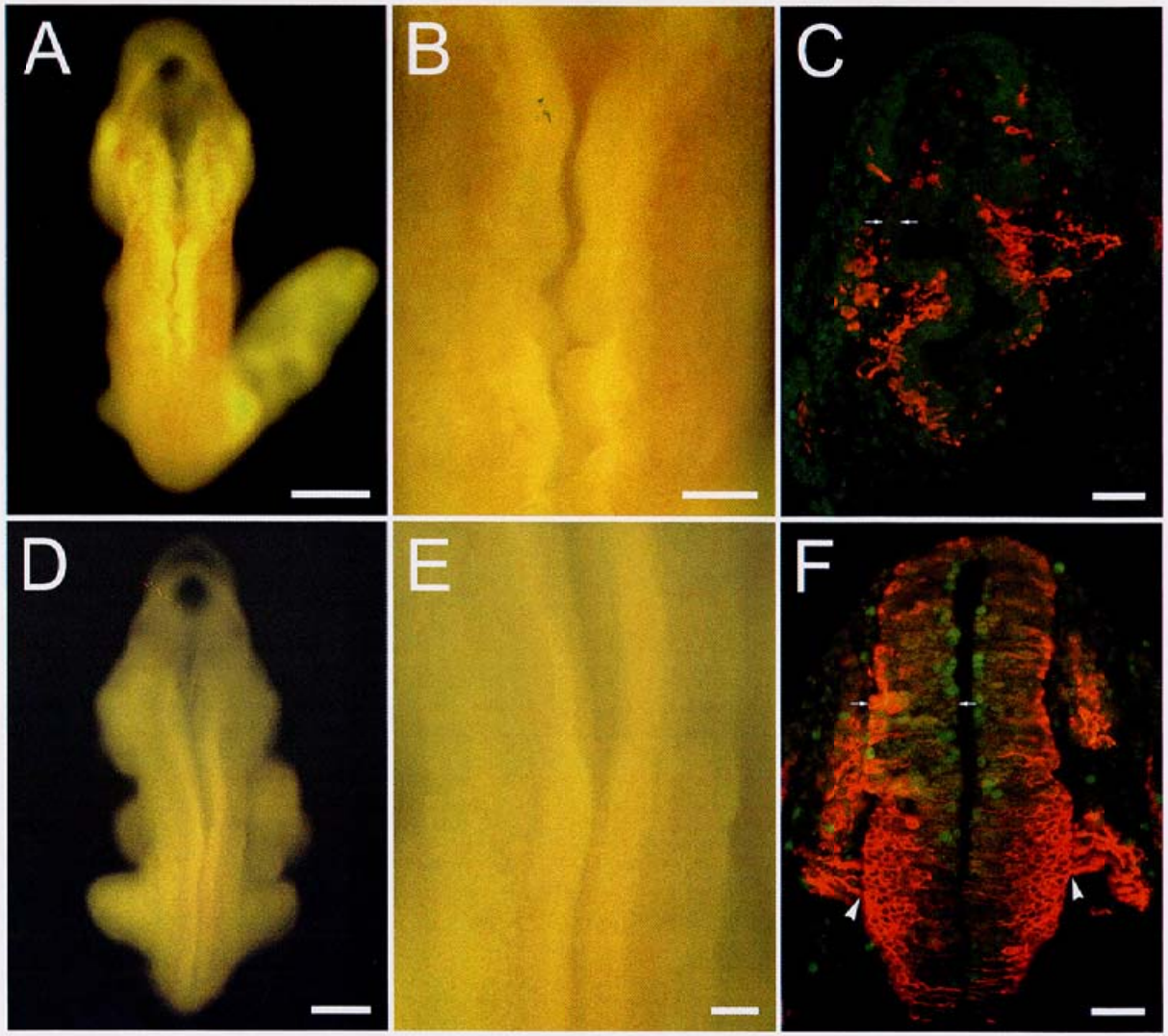

Figure. 4

Table 1
Characterization of neural cell types used for cloning

Ages of donor cells	N =	No. of cells tested	No. (%)* of NeuN (+) cells
P0	2	11	11 (100)
P1	2	6	6 (100)
P2	2	7	7 (100)
P3	2	7	7 (100)
P4	1	3	3 (100)
Total	9	34	34 (100)

Note. *Percentage of NeuN-positive cells in the cells tested.

Table 2
Generation of live-born pups using the nuclei of neurons collected from the cerebral cortex at P0-P4

Donor cells	No. of reconstructed oocytes	No. (%)*of oocytes activated	No. (%)§ of molurae/ blastcysts	No. of embryos transferred	No. (%)§ newborn pups	No. (%)§ pups developed into adults
Neurons	184	84 (45.7)	17 (20.2)	17	0 (0)	0 (0)
Cumulus cells	132	77 (58.3)	42 (54.5)	42	3 (3.9)	2 (2.6)

Note. *Percentage of oocytes with a pronucleus after activation.
§Percentage of embryos or pups that developed from activated oocytes.

Table 3
Mouse cloning using nuclei of neurons collected from the cerebral cortex at P0-P4

Donor cells	No. of reconstructed oocytes	No. (%)* of oocytes activated	No. (%)§ of molurae/ blastcysts	No. of embryos transferred	Total no. (%)§ of fetuses	No. (%)§ normal fetuses
Neurons	423	307 (72.6)	-	295	22 (7.2)	2 (0.7)
	971	593 (61.1)	237 (40.0)	231	18 (3.0)	0 (0)
	1394	900 (64.6)	-	526	40 (4.4)	2 (0.2)
Cumulus cells	105	87 (82.9)	-	87	5 (5.7)	3 (3.4)

Note. *Percentage of fetuses that developed from reconstructed oocytes. §Percentage of fetuses that developed from activated oocytes.

Table 4
Morphological features of abnormal fetuses cloned with nuclei of neurons

Donor cells		Total no. of fetuses	No. (%)*of abnormal fetuses	No. (%)§of abnormal fetuses that did not display				Average of C-R length (average±S.D) (mm)
name	age			heartbeat	closed neural tube	turning	forelimb buds & hindlimb buds	
Neurons	P0	8	7 (87.5)	6 (85.7)	6 (85.7)	1 (14.3)	7 (100)	2.12±0.74
	P1	14	13 (92.9)	10 (76.9)	10 (76.9)	2 (15.4)	13 (100)	2.39±0.74
	P2	14	14 (100)	9 (64.3)	11 (78.6)	2 (14.3)	14 (100)	2.48±0.65
	P3	1	1 (100)	1 (100)	1 (100)	1 (100)	1 (100)	(2.50)
	P4	3	3 (100)	3 (100)	3 (100)	0 (0)	3 (100)	2.55±0.45
	Total	40	38 (95.0)	29 (76.3)	31 (81.6)	6 (15.8)	38 (100)	2.42±0.71
Cumulus cells		5	2 (40.0)	1 (50.0)	1 (50.0)	1 (50.0)	2 (100)	1.60

Note. *Percentage of abnormal fetuses among total fetuses. §Percentage of abnormal fetuses displaying each characteristic.

Chapter 2

Chimeras of wild-type embryos and embryos cloned using nuclei from differentiated neurons display neural abnormalities

Abstract

Neither adult nor fetal mice have ever been obtained by cloning when the nuclei of adult neurons from the cerebral cortex were used. In contrast, I have successfully produced cloned mice using the nuclei of fetal neural cells from the cerebral cortex. Moreover, when the nuclei of differentiated neurons from the cerebral cortex of postnatal day 0 to 4 mice are used for cloning, the cloned fetuses display neural abnormalities, with disorganization at the cytoarchitectural level and an irregular distribution of neurons. To assess the abnormal neural development in fetuses cloned using the nuclei of differentiated neurons, I generated chimeric mice by aggregating cells from cloned and wild-type embryos. Cells that were derived from the cloned embryos differentiated into hair cells in the one adult mouse I obtained. To readily identify cells that were derived from the cloned embryos, I adopted a technique of making chimeras from cloned embryos that expressed the *lacZ* gene aggregated with wild-type embryos. The LacZ-positive cells differentiated into normal cells of the proximal renal tubules in the single chimeric pup, and contributed to tissues derived from all three germ layers in the chimeric fetuses. Chimeric fetuses that contained large numbers of LacZ-positive cells showed severe growth retardation. The chimeric fetuses with a small number of LacZ-positive cells displayed neural abnormalities that included collapsed regions in the neural tube lumen and ventricular surfaces of the neuroepithelium. These collapsed structures were lined by both LacZ-positive and wild-type cells. Isolated LacZ-positive cells in the neural tissues of chimeric fetuses had abnormalities that included denucleation and aggregation of nuclei. Thus, chimeric fetuses demonstrated neural abnormalities at the cytoarchitectural and single-cell levels. These results indicated that cells cloned from the nuclei of differentiated neurons could contribute to tissues derived

from the three embryonic germ cell layers, but could not differentiate into normal neural cells. My results support the idea that the nuclei of differentiated neurons are not totipotent and cannot fully drive normal development.

Introduction

Mammals can now be cloned using somatic cells. Although various types of somatic cells have been used successfully to direct full-term development (Solter, 2000; Tsunoda and Kato, 2002; Wakayama and Yanagimachi, 2001), no one has successfully cloned mice from the nuclei of adult neurons (Wakayama et al., 1998; Osada et al., 2002). When premature and just-differentiated neural cells derived from mouse cerebral cortex at 15.5 days postcoitum (dpc) were used as nuclear donors, healthy cloned mice and fetuses were obtained (Yamazaki et al., 2001). In contrast, nuclei of postmitotic differentiated neurons from the mouse cerebral cortex at 17.5 dpc produced cloned pups and cloned fetuses, but the majority of the cloned fetuses had an abnormal neural tube with internal protrusions and dispersed cells (Yamazaki et al., 2001). In addition, when the nuclei of NeuN-positive differentiated neurons from the cerebral cortex of postnatal day 0 to 4 mice were used for cloning, no cloned neonatal mice were obtained. The majority of cloned fetuses produced using the nuclei of differentiated neurons exhibited morphological neural defects (Chapter 1). The distribution patterns of markers for neurons and proliferating cells were abnormal or the markers were absent from the neural tissues of these cloned fetuses. Taken together, these reports indicate that the nuclei of neurons do not have the developmental potential to drive differentiation into normal neural cells, and, in fact, if the nuclei are taken from postnatal day (P) 0 to 4 mouse cerebral cortex, they are embryonically lethal.

To elucidate the developmental potential of nuclei derived from differentiated neurons, I wished to investigate their fate at the single-cell level. To do this, I needed to rescue the embryos from the embryonic lethality of the cloned postmitotic neuronal nuclei. The generation of aggregation chimeras is a strategy that has been used to

elucidate the mechanisms responsible for defects in the gene-targeted mice with severe embryonic abnormalities, or that die as embryos or soon after birth, by rescuing the embryos from the defects caused by the targeted genes (Rivera-Pérez et al., 1999; Neganova et al., 2000; Maskos and McKay, 2003). Therefore, in an attempt to rescue the embryonic lethality associated with cloning from differentiated neuronal nuclei, and to assess the developmental potential of individual cloned cells, I made chimeric mice by aggregating wild-type embryos and embryos that were cloned using the nuclei of differentiated neurons.

In this paper, I also adopted the technique of using cryopreserved wild-type embryos to produce aggregation chimeras efficiently, since the right number of wild-type embryos at the appropriate developmental stage must be available when the cloned embryos are ready. This was necessary because wild-type embryos and embryos cloned with somatic cell nuclei do not follow the same pace of development (my preliminary data). In fact, embryos that are cloned from the nuclei of neurons display developmental retardation even before implantation.

Cryopreservation has been used to preserve wild-type mouse embryos and to prepare for the efficient generation of chimeric mice. Previous studies have pointed out several risks of cryopreservation, such as an increased risk of abnormalities, as well as other risks, including enzyme inactivation (Rammler, 1967; Fahy, 1986; Carpenter and Crowe, 1988), ionic disturbances, attack by free radicals (Alvarez and Storey, 1992; Petrenko, 1992; Whiteley et al., 1992), damage to the genetic material (Shaw et al., 1991; Bouquet et al., 1993), and effects on morphophysiology and behavior (Dulioust et al., 1995). However, recent studies have succeeded in reducing those risks by using new methods and reagents (Nakagata, 1989, 1990 and 2001).

Here, I a successfully obtained a chimeric pup, a chimeric mouse, and chimeric fetuses. The chimeric mouse had agouti hairs derived from cloned embryos. The chimeric pup died soon after birth, and contained cells derived from cloned embryos incorporated into the proximal renal tubules. In the chimeric fetuses, cells from the cloned animals were found in all three germ cell layers. These cells exhibited abnormalities, including aggregation of nuclei and denucleation in the neural tissues.

This study showed that cells derived from embryos cloned using the nuclei of differentiated neurons contributed to the three embryonic germ cell layers but failed to develop into normal neural cells. My results suggest that the nuclei of differentiated neurons retain insufficient potential to direct differentiation into new normal neural cells.

Materials and methods

Mice

Homozygous C57BL/6J-Gtrosa26 (C57BL/6-TgR[ROSA26]26Sor) (ROSA26) males and C57BL/6J females were purchased from the Jackson Laboratory (Bar Harbor, ME). Wild-type B6D2F1 females for oocyte collection and DBA/2 males were purchased from the National Cancer Institute (Frederick, MD). CD-1 mice were obtained from Charles River (Wilmington, MA). ROSA26 has a β-galactosidase (β-gal) construct (Friedrich and Soriano, 1991) on both alleles. Pups heterozygous for the β-gal construct were generated by the natural mating of (C57BL/6J X ROSA26) F1 females with DBA/2 males. These pups are denoted as "ROSAHt". ROSA26 heterozygotes do not display an overt phenotype and are fertile, as are the homozygotes (Zambrowicz et al, 1997). The ubiquitous expression of β-gal is found in heterozygous newborns, with background staining in the intestines (Zambrowicz et al, 1997). All neuronal and glial cell types within the cerebral cortex are also LacZ-positive (my preliminary data). To obtain B6D2F1 fetuses and pups, C57BL/6J females were mated to DBA/2 males. The day the vaginal plug was observed was designated as 0.5 days postcoitum (dpc). The day the pup was born was designated as P0. To obtain unfertilized oocytes for cloning, B6D2F1 females were induced to superovulate by intraperitoneal injections of 5 IU PMSG and then 5 IU hCG 48 hours later. To acquire wild-type embryos at the 2-cell stage, C57BL/6J and CD-1 females were induced to superovulate as above. The C57BL/6J females were then mated to DBA/2 males and the CD-1 females were mated to CD-1 males. Both B6D2F1 and CD-1 embryos used for aggregation are described as wild-type embryos in this paper. All the mice were bred in the animal facilities under a

14h/10h light/dark cycle. They were maintained at the University of Hawaii at Manoa Laboratory Animal Service. The guidelines of the respective Animal Care and Use Committees were followed. Fetuses at 10.5 dpc are called "fetuses" in this study.

Preparation of Donor Cells for Cloning

Differentiated neurons were collected from wild-type B6D2F1 and ROSAHt pups at P0-P4 for cloning. The isolation and characterization of differentiated neurons was as previously described (Chapter 1). The nuclei of the differentiated neurons in the mouse cerebral cortex at P0-P4 are denoted as "DNn."

Nuclear Transfer and Oocyte Activation

The generation of cloned mice with DNn was carried out as previously described (Chapter 1). Embryos, fetuses, mice, and cells that contained DNn are denoted as "DNnt embryos," "DNnt fetuses," "DNnt mice," and "DNnt cells," respectively.

Generation of Aggregation Chimeras

The zona pellucida of embryos at the 4- to 8-cell stage was removed with 0.5% pronase (KAKEN PHARMACEUTICAL Co., Ltd., Japan) in HEPES-CZB media for 3 min at 37°C. A single DNnt embryo at the 4- to 8-cell stage was cultured with a single wild-type embryo at the 4- to 8-cell stage in mini-wells that were created with a Hungarian darning needle (Wood et al., 1993). Aggregates that were constructed with one DNnt embryo and one wild-type embryo are called DNnt aggregates. Twenty-four hours after aggregation, DNnt aggregates developed into blastocysts called "aggregated blastocysts." Aggregated blastocysts were transferred into recipient CD-1 females. Any

chimeric fetus, pup, or mouse made from a DNnt and a wild-type embryo is called a "DNnt chimeric fetus", "DNnt chimeric pup," and "DNnt chimeric mouse," respectively.

Cryopreservation of 2-cell stage Embryos

The cryopreserving and thawing of embryos at the 2-cell stage was carried out with a slight modification of a previously described method (Nakagata, 1989 and 1990). Forty-five to 46 hours after the hCG injection, embryos at the 2-cell stage were flushed from the oviduct with HEPES-CZB media, and then cryopreserved. Wild-type embryos that were thawed after freezing are called "Freeze&Thaw embryos." In this paper, Freeze&Thaw embryos were used to generate aggregation chimeras with DNnt embryos.

Embryo Transfer

Cloned embryos were transferred as previously described (Chapter 1). DNnt blastocysts that had developed 1 day after aggregation were transferred into the uterine horn of day 2 pseudo-pregnant CD-1 surrogate females. Term fetuses were obtained by Cesarean section, and they were raised by lactating foster CD-1 mothers.

5-Bromo-4-Chloro-3-Indolyl β-D-Galactoside (X-gal) Staining

For β-gal detection, DNnt chimeric fetuses or the cerebral cortex of the postnatal ROSAHt pups were rinsed in 0.1 M phosphate buffer (PB) and then fixed in 2% formaldehyde, 0.2% glutaraldehyde for 30 min at 4°C. The specimens were rinsed three times with rinse buffer, which contained 0.02% NP40, 2 mM $MgCl_2$ and 0.01%

deoxycholic acid in 0.1 M PB, for 20 min at room temperature. They were then stained in a reaction mixture containing 1 mg/ml X-gal in dimethyl formamide, 5 mM potassium ferricyanide, and 5 mM potassium ferrocyanide in the rinse buffer for 24-48 hours at 37°C. Images were viewed with an OLYMPUS SZX12 microscope and recorded on Elite CHROME ASA100 (KODAK) with an OLYMPUS PM30 EXPOSURE CONTROL UNIT. They were then scanned and processed electronically.

Histochemistry

The X-gal-stained specimens were washed briefly in 0.1 M PB, and they were postfixed in 4% paraformaldehyde in 0.1 M PB overnight at 4°C for histological analysis. After the fixation step, they were rinsed with 0.1 M PB, and washed extensively in 70% ethyl alcohol. They were then dehydrated by serial passage through graded ethyl alcohol solutions (70%, 90%, 100%, and 100%) followed by immersion in xylene. Samples were placed in a 1:1 mixture of xylene and paraffin for 30 min to 1 hr at 61°C. They were then incubated twice in paraffin, first for 1 hr and second for 1 to 4 hrs, each at 61°C. After the specimens were embedded, 10-μm-thick sections were cut. For Feulgen staining, specimens were dewaxed, washed in running tap water for 10 min, and rinsed in distilled water for 2 min. They were then treated with 1 N HCl for 10 min at 60°C, washed twice in 1 N HCl, rinsed in distilled water for 5 min, and then stained in Schiff reagent for 10 min. They were then treated with a sulfurous acidic solution 3 times for 3 min each. Finally, they were washed in running tap water for 20 min. All sections were dehydrated by serial passage through graded ethyl alcohol solutions, as above. Coverslips were applied with Permount (Fisher Scientific), and the mounted sections were examined with an OLYMPUS BX51 microscope. The images were

recorded with an OLYMPUS DP50-CU digital camera and processed electronically.

Results

Effective strategy for producing aggregation chimeras from DNnt and wild-type embryos

To elucidate the developmental potential of DNnt cells, I generated DNnt chimeras by combining DNnt and wild-type embryos.

First, the developmental potential of wild-type embryos was examined. Wild-type embryos without a zona pellucida developed into normal fetuses (data not shown, 86.1% of embryos transferred) and healthy pups (data not shown, 34.0% of embryos transferred). Aggregates that were constructed with two wild-type embryos developed normally as fetuses (data not shown, 58.0% of embryos transferred) and were born as healthy pups (data not shown, 21.2% of embryos transferred).

When I used differentiated neural cell nuclei (DNn) for cloning, I obtained activated oocytes (data not shown, 85.0% of reconstructed oocytes) and 4- to 8-cell stage DNnt embryos (data not shown, 39.8% of activated oocytes). DNnt embryos without a zona pellucida at the 4- to 8-cell stage tended to form isolated blastomeres. No fetus was obtained from these embryos.

Twenty-six DNnt aggregates that were made from DNnt and wild-type embryos developed into 11 aggregated blastocysts (42.3% of DNnt aggregates) ("Fresh," Table 1). The developmental pace of embryos cloned using somatic cell nuclei was different from that of wild-type embryos (my preliminary data). Moreover, DNnt embryos also developed with an irregular time schedule that was different from that of wild-type embryos (my preliminary data). This made it difficult to prepare enough wild-type embryos at the appropriate developmental stage to produce DNnt chimeric embryos.

Therefore, I decided to try using wild-type embryos that were thawed after cryopreservation (Freeze&Thaw embryos) to produce DNnt chimeric mice efficiently.

Single Freeze&Thaw embryos developed into normal fetuses (data not shown, 74.1% of embryos transferred) and healthy pups (data not shown, 40.9% of embryos transferred). Aggregates that were constructed with two Freeze&Thaw embryos developed into normal fetuses (data not shown, 49.2% of embryos transferred). One hundred and thirty DNnt aggregates made from DNnt embryos and Freeze&Thaw embryos developed into 72 aggregated blastocysts (55.4% of DNnt aggregates) ("Freeze&Thaw," Table 1). As these results indicated that the efficiency of producing aggregated blastocysts using Freeze&Thaw embryos was higher than that of using fresh embryos (Table 1), I adopted the use of Freeze&Thaw wild-type embryos to produce DNnt aggregates. My strategies for generating DNnt chimeric fetuses and mice using DNnt embryos that had a *lacZ* reporter gene and Freeze&Thaw embryos are summarized in Fig. 1.

Production of DNnt chimeric mice

Using Freeze&Thaw embryos that were derived from CD-1 would permit us to identify the presence of DNnt cells, which would produce agouti hair that would be visible against the genetic background of the donor mice. I produced 380 activated oocytes (81.0% of reconstructed oocytes, Table 2(1)). Fifty-four DNnt embryos at the 4- to 8-cell stage were aggregated with Freeze&Thaw embryos, and they developed into 37 aggregated blastocysts (68.5% of DNnt aggregates, Table 2(1)). Twenty-seven mice were obtained (5.8% of reconstructed oocytes, Table 2(1)), and 1 of them had agouti hairs derived from DNnt cells on his back (Fig. 2, arrow; 0.2% of reconstructed oocytes,

Table 2). When I crossed this DNnt chimeric male to wild-type CD-1 females, over 100 descendants without agouti hairs were produced. This result suggested that DNnt cells did not differentiate into sperm cells in this chimera. Further experiments using H-E and Nissl staining of the brain in the DNnt chimeric male at P106 showed no histological abnormality.

Histological analysis of DNnt chimeric pups

To identify DNnt cells in DNnt chimeric mice, I used ROSAHt mice at P0-P4 for cloning. If I used nuclei from differentiated neurons of ROSAHt mice as donor nuclei, I could detect DNnt cells as LacZ-positive cells in the DNnt chimeric mice. I produced 247 activated oocytes (83.2% of reconstructed oocytes, Table 2(2)). Nineteen DNnt embryos at the 4- to 8-cell stage aggregated with Freeze&Thaw embryos, and they developed into three aggregated blastocysts (15.8% of DNnt aggregates, Table 2(2)). Eight pups were acquired (2.7% of reconstructed oocytes, Table 2(2)). One pup was dying at P1, so I dissected and stained her tissues including the tail, skin, thymus, lung, heart, liver, stomach, spleen, pancreas, a series of intestinal pieces, adrenal gland, kidney, bladder, cerebral cortex, and olfactory bulbs with X-gal to identify LacZ-positive cells. This pup had LacZ-positive cells in the proximal renal tubules of her kidneys (Fig. 3B, asterisks; 0.3% of reconstructed oocytes, Table 2(2)) and in her tail. The nuclei of the LacZ-positive cells in the proximal renal tubules were not detectably abnormal. The remaining tissues did not have LacZ-positive cells. I also sacrificed the remaining seven healthy pups at P1, and found no LacZ-positive cells in their tissues nor any histological abnormalities. These results demonstrated that DNnt cells could differentiate into at least some postnatal mouse tissues.

Generation of DNnt chimeric fetuses

The surrogate mothers with the transferred aggregated blastocysts often lost weight between 9.5 and 11.5 dpc, suggesting that DNnt chimeric fetuses were apt to die during embryogenesis. I attempted to generate DNnt chimeric fetuses at 10.5 dpc to assess the developmental potential of each DNnt cell.

I succeeded in producing 114 activated oocytes (84.4% of reconstructed oocytes, Table 3). Eighty-one DNnt embryos at the 4- to 8-cell stage were aggregated with Freeze&Thaw embryos at the 4- to 8-cell stage, and they developed into 34 aggregated blastocysts (42.0% of DNnt aggregates, Table 3). Twenty-six fetuses were obtained (19.3% of reconstructed oocytes, Table 3), and 5 of them contained LacZ-positive cells (3.7% of reconstructed oocytes, Table 3). The five DNnt chimeric fetuses were termed CH 1 (Table 4), CH2 (Table 4), CH3 (Figs. 4A and 4D, Table 4), CH4 (Figs. 4B and 4E, Table 4), and CH5 (Figs. 4C and 4F, Table 4), respectively.

I analyzed these fetuses by comparing features of their development with those of wild-type mice. In wild-type fetuses, the embryos show "turning" between 8.5-9.0 dpc, develop forelimb buds between 9.5-10.25 dpc, and show neuropore closure and the development of hindlimb buds between 10.25-10.75 dpc (Kaufman, 2002). The heartbeat is also visible in normal wild-type embryos at these stages. Here, I defined normal fetuses as those that met four criteria: heartbeat, normal closing of the neural tube, turning, and both forelimb and hindlimb buds.

Both CH1 and CH2 were smaller than 1.0 mm and showed severe developmental retardation (Table 4). They displayed strong X-gal staining throughout their bodies (Table 4). Thus, CH1 and CH2 were not rescued from embryonic abnormalities. CH5

had a large number of LacZ-positive cells (Figs. 4C and 4F; Table 4), no blood, no heartbeat, a distended pericardial cavity (arrowhead, Fig. 4C), and developmental retardation (Figs. 4C and 4F; Table 4). Thus, CH5 was also not rescued from embryonic abnormalities. In contrast, CH3 (Fig. 4A and 4D) and CH4 (Fig. 4B and 4E), which had few LacZ-positive cells, had strong blood flow and a heartbeat (Table 4). They appeared to be normal by the other criteria as well (1.5% of reconstructed oocytes, Tables 3 and 4). Thus, DNnt chimeric fetuses that contained a small number of LacZ-positive cells were rescued from developmental retardation. Interestingly, not only the body of DNnt chimeric fetuses, but also their yolk sacs contained LacZ-positive cells in mosaic patterns (arrow, Fig. 4A). I produced two kinds of aggregates as control embryos. One was made from a ROSAHt embryo and a wild-type embryo, and the other from a ROSAHt embryo and a Freeze&Thaw embryo (Fig. 5A and 5B). Both developed into normal fetuses at high frequency (data not shown). My results demonstrated that DNnt cells held the developmental potential to be incorporated into fetal tissues, and they disturbed the normal development of wild-type cells in the chimeras that harbored a large number of them.

Contribution of DNnt cells to the DNnt chimeric fetuses

To understand the contribution of the DNnt cells to the DNnt chimeric fetuses, I made paraffin sections of CH3, CH4, and CH5. LacZ-positive cells were observed in various tissues of these DNnt chimeric fetuses, including the lens, neuroepithelium (Fig. 5C-5F), neural tube (Fig. 6A and 6B), inner (neural) layer of the optic cup (Fig. 6C and 6D), dorsal root ganglion (DRG), heart (Fig. 6E and 6F), somite, limb bud (Fig. 6G and 6H),

mesenchyme, branchial arch, and hind gut (Table 5). These results indicated that DNnt cells could contribute to tissues that were derived from all three germ cell layers.

Histological analysis of DNnt chimeric fetuses

As DNnt fetuses had morphological defects in their neural tissues (Chapter 1), I first examined the contribution of the DNnt cells to the neural tissues. I generated chimeric fetuses from a single ROSAHt embryo and a single Freeze&Thaw embryo, as controls (Fig. 5A and 5B). The control chimeric fetuses did not show any morphological abnormalities (Fig. 5B). Both wild-type (small arrows, Fig. 5B) and LacZ-positive cells (large arrows, Fig. 5B) had nuclei that showed no notable abnormality. In the telencephalic neuroepithelium of the chimeric fetuses, LacZ-positive cells were widely dispersed (Fig. 5).

To understand the original developmental potential of single DNnt cells in the DNnt chimeric fetuses, I examined the morphological features of the normal DNnt chimeric fetuses, CH3 and CH4. The neuroepithelium of CH3 did not have any remarkable morphological abnormalities. In the same region, LacZ-positive cells displayed denucleation (arrowheads, Fig. 5D). Furthermore, clusters of LacZ-positive cells were observed in the mesenchymal tissues neighboring the neuroepithelium (a large arrow, Fig. 5D).

In CH4, the ventricular surfaces of the neuroepithelium were intermittently disrupted (double-headed arrows, Fig. 5E), and near the ventricular surface of the neuroepithelium, the LacZ-positive cells frequently showed denucleation (arrowhead, Fig. 5F) and aggregation of their nuclei (large arrows, Fig. 5F). At the ventricular surface of the neuroepithelium of CH3 as well, the DNnt cells had abnormalities that included

denucleation and the aggregation of nuclei. I also noted that in the other chimeric fetuses, which contained a large number of LacZ-positive cells, even the wild-type cells showed abnormalities (data not shown).

To assess the abnormalities of the chimeric fetuses in detail, I examined the morphological features of CH3, which was normal in appearance. The lumen of neural tube near the tail was disrupted (double-headed arrows, Fig. 6A). Both DNnt cells (large arrows, Fig. 6B) and wild-type cells (small arrows, Fig. 6B) near the surface of the lumen were separated from neighboring cells. A similar phenomenon was observed in the neural tube of CH4 and CH5 (data not shown). LacZ-positive cells without nuclei did not contact peripheral cells tightly (an arrowhead, Fig. 6B). The ventricular surface of the inner (neural) layer (In, Fig. 6C) and outer layer of the optic cup did not have remarkable histological defects (Ou, Fig. 6C). In addition, the LacZ-positive (large arrows, Fig. 6D) and wild-type cells (a small arrow, Fig. 6D) in the ventricular surface of the inner layer of the optic cup and the wild-type cells (an asterisk, Fig. 6D) in the outer layer of the optic cup had normal nuclei.

LacZ-positive cells were also found in the mandibular component of first branchial arch (Ma, Fig. 6E), the truncus arteriosus region (Ta, Fig. 6E), the common atrial chamber of heart (Ac, Fig. 6E), the bulbus cordis (Bc, Fig. 6E), the hepatic/biliary primordial within septum transversum (H/Bp, Fig. 6E), and the forelimb and hindlimb buds (Fig. 6G). In those tissues, no remarkable morphological abnormalities were observed (Fig. 6E and 6G), and both the LacZ-positive (large arrows, Fig. 6F and 6H) and wild-type cells (small arrows, Fig. 6F and 6H) had normal nuclei. Thus, a histological analysis of CH3 showed that even chimeric fetuses that were apparently normal carried morphological abnormalities in their neural tissues. Furthermore,

LacZ-positive neural cells lost their nuclei and both DNnt and wild-type neural cells were separated from adjacent tissues.

Discussion

I studied the developmental potential of DNnt cells in chimeric embryos. Overcoming a technical difficulty, I found that wild-type embryos that had been thawed after cryopreservation at the 2-cell stage could be used to generate DNnt chimeric embryos efficiently. DNnt cells differentiated into hair cells and proximal renal tubule cells in these postnatal DNnt chimeric mice. In the DNnt chimeric fetuses, the DNnt cells contributed to tissues that were derived from all three germ cell layers. DNnt chimeric fetuses had morphological abnormalities including collapsed regions of the neural tube lumen and ventricular surfaces of the neuroepithelium. In these structures, both DNnt and wild-type cells were likely to separate from adjacent tissues and the DNnt cells often lost their nuclei.

Features of DNnt embryos during early embryogenesis

It has been reported that Freeze&Thaw embryos at the 8-cell stage without a zona pellucida produce aggregated blastocysts with high frequency (around 80% of aggregates) with the same kind of embryos (Landa and Tepla, 1990). Wild-type embryos have been used to generate chimeric embryos to understand the function of genes including *Goosecoid* (Rivera-Pérez at al., 1999), *Dct* (a marker gene for melanoblasts; (Wilkie et al., 2002), and *E-cadherin* (Neganova et al., 2000). In all of these studies, the Freeze&Thaw embryos produced normal fetuses.

DNnt embryos at the 4- to 6-cell stage dissociated into single blastomeres soon after their zona pellucida was removed (my preliminary data). Even though chimeras made from two wild-type embryos or two Freeze&Thaw embryos generated aggregated

oocytes efficiently (my preliminary data), aggregates made with a DNnt and a wild-type embryo failed to produce DNnt chimeric blastocysts at a high frequency. In addition, aggregates made from one wild-type and one Freeze&Thaw embryo became aggregated blastocysts with the frequency seen for aggregates made from 2 Freeze&Thaw embryos.

My results demonstrate that the blastomeres of DNnt embryos have less ability to adhere to one another than do those of either wild-type or Freeze&Thaw embryos. It has been suggested that dynamic changes in the expression of adhesion molecules may be important for the interaction of the embryo with the maternal cellular environment, as well as for the continuing development and survival of the early embryo (Lu et al., 2002). Uvomorulin (E-cadherin), which is the major cell adhesion molecule responsible for intercellular adhesion in early mouse embryos, is required when pronuclear formation occurs (Clayton et al., 1993) and during mouse preimplantation (Ohsugi et al., 1999; Vestweber et al., 1985). Previous papers have demonstrated that it is necessary for the E-cadherin adhesion complex to be expressed at the appropriate place and time in blastomeres for normal mouse development to proceed. These previous findings lead us to hypothesize that insufficient expression of E-cadherin at the junction between the blastomeres of DNnt embryos is one of the reasons for the abnormal development of DNnt embryos and DNnt chimeric embryos.

DNnt cells in the tissues of DNnt chimeric mice

When neurons derived from adult mouse cerebral cortex were used for cloning, neither cloned mice nor fetuses were produced (Wakayama et al., 1998; Osada et al., 2002). When I attempted to generate cloned mice using the nuclei of NeuN-positive differentiated neurons from the cerebral cortex of postnatal day 0 to 4 mice, I did not

obtain any cloned mice. However, I succeeded in producing cloned fetuses at 10.5 dpc that frequently had morphological abnormalities in their neural tissues (Chapter 1). Moreover, embryos that were cloned using the nuclei of postmitotic differentiated neurons from the 17.5 dpc cerebral cortex usually failed to become healthy fetuses or pups (Yamazaki et al., 2001). Thus, the nuclei of neurons have not been able to drive normal development in cloned embryos. Although DNnt cells were detected in the DNnt chimeric mice, the contribution of these cells was small (arrow, Fig. 2 and asterisks in Fig. 3B, Table 2). Only 2 of 35 total mice were chimeric (5.7% of all mice obtained, Table 2). The rates for generating mice (4.6% of reconstructed oocytes) and DNnt chimeric mice (0.3% of reconstructed oocytes) were similar to the rates for producing DNnt fetuses (4.4% of reconstructed oocytes) and normal DNnt fetuses (0.2% of reconstructed oocytes) (Chapter 1). This resemblance suggests that DNns do not retain sufficient developmental potential to drive normal development, even in the context of a chimeric animal containing many wild-type cells.

In this paper, I found that LacZ-positive DNnt cells differentiated into hair cells (arrow, Fig. 2) and cells contributing to the proximal renal tubules (asterisks in Fig. 3B) of DNnt chimeric mice. These results are the first demonstration at the cellular level that cells derived from DNnt embryos have the developmental potential to differentiate into postnatal mouse tissues.

Abnormalities of DNnt chimeric fetuses at 10.5 dpc

Fetuses cloned from postmitotic differentiated neural nuclei have neural abnormalities such as undulating neural tubes, protrusions of the neural epithelium into the cerebral lumen of the fourth ventricle, collapsed lumen of the spinal cord, and

loosely compacted cells in the abnormal neural tube (Yamazaki et al., 2001). DNnt fetuses also have several neural abnormalities (Chapter 1): e.g., open anterior neuropore, undulating neural tube closure, neuroepithelium of an uneven thickness, and a collapsed ventricular surface of the neuroepithelium and collapsed lumen of the neural tube.

In the DNnt chimeric fetuses, DNnt cells had notably abnormal nuclei in the neural tissues (Fig. 5E and 5F, Fig. 6B), and these cells were likely to be segregated from peripheral tissues (large arrows, Fig. 5F, Fig. 6B). Moreover, DNnt chimeric fetuses that contained large numbers of the LacZ-positive DNnt cells exhibited severe developmental retardation (Fig. 4C and 4F, Table 4). Thus, my results indicate that neural abnormalities in chimeric DNnt fetuses are similar to those seen in fetuses cloned with postmitotic differentiated neural cells and in DNnt fetuses, and they suggest that it is difficult for DNnt cells to differentiate into normal neural cells. In contrast, control embryos developed into normal fetuses with no abnormal nuclei (Fig. 5A and 5B). Interestingly, the LacZ-positive DNnt cells did not show remarkable abnormalities in non-neural tissues, and the only normal-appearing neural tissues were those of CH3, which contained only a small number of LacZ-positive cells. These results indicate that DNnt cells did not have the necessary developmental potential to differentiate into neurons; rather, they had nuclear abnormalities that were detectable at the single-cell level.

The ventricular and subventricular zones in the neuroepithelium of normal fetuses are important in regulating the regional specification and differential growth of the prosencephalic primordia (Rossant and Tam, 2002). These areas contain mitotically active cells, whereas the postmitotic zone, including the marginal zone, contains predominantly postmitotic cells (Rossant and Tam, 2002). Neural progenitor cells in the

neural tube proliferate in a layer that is adjacent to the lumen. When progenitor cells become postmitotic, they migrate to the differentiation zone that lies under the pial surface; other cells that leave the ventricular zone remain mitotically active and enter the subventricular zone (Rossant and Tam, 2002). Here I noted that DNnt cells tended to be dissociated from adjacent cells in the neural tissues. This dissociation suggests a reduction in the adherent ability of DNnt cells in the DNnt chimeric fetuses. This probably originates with the downregulation of adhesion-related genes and/or the lack of adhesion molecules, and is consistent with the dissociation I observed in the DNnt blastocysts.

Evaluation of abnormalities in the DNnt cells

Cells in the neural tubes of abnormal fetuses that are cloned using the nuclei of postmitotic differentiated neural cells show aggregation of their nuclei (my preliminary data; Yamazaki et al., 2001). Some cells in the neuroepithelium of the growth-retarded DNnt fetuses show pyknosis (data not shown; Chapter 1). DNnt cells showed denucleation in the neural tissues of DNnt chimeric fetuses (arrowheads, Fig. 5D and 5F, Fig. 6B). These results demonstrate that it was difficult for these cells, even though they contained the clone of a nucleus that had driven the differentiation of its original cell to become a neuron, to become normal neurons themselves.

When embryos that were cloned using the nuclei of Purkinje cells derived from mice older than 8 weeks show evidence of chromosomal disorders, their development stops at the 2-cell stage (Osada et al., 2002). In addition, a recent paper reports that lagging chromosomes, supernumerary centrosomes, and non-disjunction contribute to the generation of aneuploidy among neural progenitor cells and that mitotic events account

mechanistically for aneuploidy and the production of genetic mosaicism during normal brain development (Yang et al., 2003). My results and those of previous reports suggest that neural cells change the characteristics of their chromosomes at the genetic and/or epigenetic level during development, which limits the ability of the nuclei cloned from them to drive the differentiation of the cloned cells into normal neurons or other neural cell types.

Another possible mechanism for the limited potential of the DNns is a parental-origin-specific gene regulation mechanism known as genomic imprinting that plays an essential role in growth and behavior by regulating the expression of two kinds of imprinted genes: the paternally and maternally expressed genes (Surani et al., 1984; McGrath and Solter, 1984; Cattanach and Kirk, 1985; Barlow et al., 1991; Bartolomei et al., 1991; DeChiara et al., 1991; Kaneko-Ishino et al., 1995; Miyoshi et al., 1998). Cloned embryos produced from 12.5 to 13.5 dpc primordial germ cells (PGCs) show growth retardation and early embryonic lethality around 9.5 dpc (Lee et al., 2002). However, cloned embryos from E11.5 PGCs survive until at least the 11.5 dpc embryonic stage (Lee et al., 2002). These authors also demonstrated that PGC clones maintained the DNA methylation status of the donor PGCs and proposed that one of the epigenetic modifications of DNA-- the differential methylation of regions of imprinted genes —induces the erasure of imprints in PGCs from 10.5 to 11.5 dpc (Lee et al., 2002).

Allele-specific methylation has been observed in all endogenous imprinted genes tested so far (Razin and Cedar, 1994), and some alleles inherit their methylation status from one gamete (Ariel et al., 1995; Kay et al., 1993; Stoger et al., 1993; Tremblay et al., 1995; Zuccotti and Monk, 1995). To date, mouse genes with brain-specific imprints,

including the calcitonin receptor gene (*Calcr*) (Hoshiya et al., 2003), the *Murr1* gene including *U2af1-rs1* gene (Nabetani et al., 1997; Wang et al., 2002; Wang et al., 2004), and the *Atp10c/pfatp* gene (Kashiwagi et al., 2003), and one gene with a brain cell type-specific imprint, *Ube3A* (Yamasaki et al., 2003), have been reported. *Calcr* is located on the proximal region of chromosome 6 and is imprinted in a tissue-specific manner, with its predominant expression being from the maternal allele in the brain. The mouse *Murr1* and *U2af1-rs1* genes are located on the proximal region of chromosome 11. Although *Murr1* is expressed biallelically in the embryonic and neonatal mouse brain, it shows maternal-dominant expression in the adult brain (Wang et al., 2004). *Ube3A* is located on chromosome 7 and encodes two RNA transcripts in the brain, a sense and antisense transcript (Yamasaki et al., 2003). The sense transcript is expressed maternally in neurons but biallelically in glial cells in the embryonic brain (Yamasaki et al., 2003); however, the antisense transcript is expressed only in neurons and only from the paternal allele (Yamasaki et al., 2003). *Atp10c/pfatp*, shows tissue-specific expression in the hippocampus and olfactory bulb (Kashiwagi et al., 2003). The data from these reports suggest that imprinted genes in the genomic DNA of neural cells are modified by epigenetic mechanisms including DNA methylation during brain development. This modification of neural genomic DNA could interfere with the ability of cloned neuronal nuclei to direct the differentiation of the DNnt cells into normal neural cells.

Analysis of genomic DNA in neurons via the establishment of ES cell lines

Neither cloned mice nor fetuses are produced from the nuclei of terminally differentiated B and T lymphocytes (Hochedlinger and Jaenisch, 2002), just as with the

nuclei of adult neurons (Wakayama et al., 1998; Osada et al., 2002). In contrast, healthy mice are generated from ES cells derived from blastocysts that were cloned using the nuclei of mature, differentiated B and T lymphocytes (Hochedlinger and Jaenisch, 2002). Moreover, healthy mice are generated from ES cells derived from blastocysts that were cloned using the nuclei of mature olfactory sensory neurons (Eggan et al., 2004; Li et al., 2004). These reports suggest that ES cells can completely reprogram their nuclei during embryogenesis. DNnt embryos do not develop into normal fetuses and healthy adults, but blastomeres can be obtained (Chapter 1).

Here I demonstrated that even at the single-cell level, DNnt cells rarely differentiated into normal neural cells in DNnt chimeric fetuses. To further analyze the developmental potential of single DNns at the genomic DNA level, I plan to establish ES cell lines derived from DNnt blastocysts. By analyzing the DNA of these ES cells throughout development, I may be able to learn more about the regulation of the genetic material of DNns. In addition, these lines may soon allow us to understand how the genomic DNA of fetal neural cells differs from that of differentiated neurons.

References

Alvarez, J. G., Storey, B. T., 1992. Evidence for increased lipid peroxidative damage and loss of superoxide dismutase activity as a mode of sublethal cryodamage to human sperm during cryopreservation. J. Androl. 13, 232-241.

Ariel, M., Robinson, E., McCarrey, J. R., Cedar, H., 1995. Gamete-specific methylation correlates with imprinting of the murine Xist gene. Nat. Genet. 9, 312-315.

Barlow, D. P., Stoger, R., Herrmann, B. G., Saito, K., Schweifer, N., 1991. The mouse insulin-like growth factor type-2 receptor is imprinted and closely linked to the Tme locus. Nature 349, 84-87.

Bartolomei, M. S., Zemel, S., Tilghman, S. M., 1991. Parental imprinting of the mouse H19 gene. Nature 351, 153-155.

Bouquet, M., Selva, J., Auroux, M., 1993. Cryopreservation of mouse oocytes: mutagenic effects in the embryo? Biol. Reprod. 49, 764-769.

Carpenter, J. F., Crowe, J. H., 1988. The mechanism of cryoprotection of proteins by solutes. Cryobiology 25, 244-255.

Cattanach, B. M., Kirk, M., 1985. Differential activity of maternally and paternally derived chromosome regions in mice. Nature 315, 496-498.

Clayton, L., Stinchcombe, S. V., Johnson, M. H., 1993. Cell surface localisation and stability of uvomorulin during early mouse development. Zygote 1, 333-344.

DeChiara, T. M., Robertson, E. J., Efstratiadis, A., 1991. Parental imprinting of the mouse insulin-like growth factor II gene. Cell 64, 849-859.

Dulioust, E., Toyama, K., Busnel, M. C., Moutier, R., Carlier, M., Marchaland, C., Ducot, B., Auroux, M., 1995. Long-term effects of embryo freezing in mice. Proc. Natl. Acad. Sci. USA 92, 589-593.

Eggan, K., Baldwin, K., Tackett, M., Osborne, J., Gogos, J., Chess, A., Axel, R., Jaenisch R., 2004. Mice cloned from olfactory sensory neurons. Nature 428, 44-49.

Fahy, G. M., 1986. The relevance of cryoprotectant "toxicity" to cryobiology. Cryobiology 23, 1-13.

Friedrich, G., Soriano, P., 1991. Promoter traps in embryonic stem cells: a genetic screen to identify and mutate developmental genes in mice. Genes Dev. 5, 1513-1523.

Hochedlinger, K., Jaenisch, R., 2002. Monoclonal mice generated by nuclear transfer from mature B and T donor cells. Nature 415, 1035-1038.

Hoshiya, H., Meguro, M., Kashiwagi, A., Okita, C., Oshimura, M., 2003. Calcr, a

brain-specific imprinted mouse calcitonin receptor gene in the imprinted cluster of the proximal region of chromosome 6. J. Hum. Genet. 48, 208-211.

Kaneko-Ishino, T., Kuroiwa, Y., Miyoshi, N., Kohda, T., Suzuki, R., Yokoyama, M., Viville, S., Barton, S. C., Ishino, F., Surani, M. A., 1995. Peg1/Mest imprinted gene on chromosome 6 identified by cDNA subtraction hybridization. Nat. Genet. 11, 52-59.

Kashiwagi, A., Meguro, M., Hoshiya, H., Haruta, M., Ishino, F., Shibahara, T., Oshimura, M., 2003. Predominant maternal expression of the mouse Atp10c in hippocampus and olfactory bulb. J. Hum. Genet. 48, 194-198.

Kaufman, H. M., 2002. The atlas of mouse development (Fifth printing of revised edition).

Kay, G. F., Penny, G. D., Patel, D., Ashworth, A., Brockdorff, N., Rastan, S., 1993. Expression of Xist during mouse development suggests a role in the initiation of X chromosome inactivation. Cell 72, 171-182.

Landa, V., Tepla, O., 1990. Construction of aggregation chimaeras from 8-cell mouse embryos stored for several years in liquid nitrogen. Folia. Biol. (Praha) 36, 159-164.

Lee, J., Inoue, K., Ono, R., Ogonuki, N., Kohda, T., Kaneko-Ishino, T., Ogura, A.,

Ishino, F., 2002. Erasing genomic imprinting memory in mouse clone embryos produced from day 11.5 primordial germ cells. Development 129, 1807-1817.

Li, J., Ishii, T., Feinstein, P., Mombaerts, P., 2004. Odorant receptor gene choice is reset by nuclear transfer from mouse olfactory sensory neurons. Nature 428, 393-399.

Lu, D. P., Tian, L., O'Neill, C., King, N. J., 2002. Regulation of cellular adhesion molecule expression in murine oocytes, peri-implantation and post-implantation embryos. Cell Res. 12, 373-383.

Maskos, U., McKay, R. D., 2003. Neural cells without functional N-Methyl-D-Aspartate (NMDA) receptors contribute extensively to normal postnatal brain development in efficiently generated chimaeric NMDA R1 -/- <--> +/+ mice. Dev. Biol. 262, 119-136.

McGrath, J., Solter, D., 1984. Completion of mouse embryogenesis requires both the maternal and paternal genomes. Cell 37, 179-183.

Miyoshi, N., Kuroiwa, Y., Kohda, T., Shitara, H., Yonekawa, H., Kawabe, T., Hasegawa, H., Barton, S. C., Surani, M. A., Kaneko-Ishino, T., Ishino, F., 1998. Identification of the Meg1/Grb10 imprinted gene on mouse proximal chromosome 11, a candidate for the Silver-Russell syndrome gene. Proc. Natl. Acad. Sci. USA 95, 1102-1107.

Nabetani, A., Hatada, I., Morisaki, H., Oshimura, M., Mukai, T., 1997. Mouse

U2af1-rs1 is a neomorphic imprinted gene. Mol. Cell Biol. 17, 789-798.

Nakagata, N., 1989. High survive rate of unfertilized mouse oocytes after vitrification. J. Reprod. Fertil. 87, 479-483.

Nakagata, N., 1990. Cryopreservation of unfertilized mouse oocytes from inbred strains by ultrarapid freezing. Experimental Animals 39, 303-305.

Nakagata, N., 2001. Procedure for simple vitrification of mouse embryos that was released officially by Center for Animal Resources and Development of Kumamoto University in Japan.

Neganova, I.E., Sekirina, G. G., Eichenlaub-Ritter, U., 2000. Surface-expressed E-cadherin, and mitochondrial and microtubule distribution in rescue of mouse embryos from 2-cell block by aggregation. Mol. Hum. Reprod. 6, 454-464.

Ohsugi, M., Butz, S., Kemler, R., 1999. Beta-catenin is a major tyrosine-phosphorylated protein during mouse oocyte maturation and preimplantation development. Dev. Dyn. 216, 168-176.

Osada, T., Kusakabe, H., Akutsu, H., Yagi, T., Yanagimachi, Y., 2002. Adult murine neurons: their chromatin and chromosome changes and failure to support embryonic development as revealed by nuclear transfer. Cytogenet. Genome Res. 97, 7-12.

Petrenko, A., 1992. A mechanism of latent cryoinjury and reparation of mitochondria. Cryobiology 29, 144-152.

Rammler, D. H., 1967. The effect of DMSO on several enzyme systems. Ann. N. Y. Acad. Sci. 141, 291-299.

Razin, A., Cedar, H., 1994. DNA methylation and genomic imprinting. Cell 77, 473-476.

Rivera-Perez, J. A., Wakamiya, M., Behringer, R. R., 1999. Goosecoid acts cell autonomously in mesenchyme-derived tissues during craniofacial development. Development 126, 3811-21.

Rossant, J., Tam, P. P. L., 2002. Patterning, regionalization, and cell differentiation in forebrain. (written by Martin, O. and Rubenstein, J. L. R.). Mouse Development (patterning, morphogenesis, and organogenesis) chapter 5, 75-105.

Shaw, J. M., Kola, I., MacFarlane, D. R., Trounson, A. O., 1991. An association between chromosomal abnormalities in rapidly frozen 2-cell mouse embryos and the ice-forming properties of the cryoprotective solution. J. Reprod. Fertil. 91, 9-18.

Solter, D., 2000. Mammalian cloning: advances and limitations. Nat. Rev. Genet. 1, 199-207.

Stoger, R., Kubicka, P., Liu, C. G., Kafri, T., Razin, A., Cedar, H., Barlow, D. P., 1993. Maternal-specific methylation of the imprinted mouse Igf2r locus identifies the expressed locus as carrying the imprinting signal. Cell 73, 61-71.

Surani, M. A., Barton, S. C., Norris, M. L., 1984. Development of reconstituted mouse eggs suggests imprinting of the genome during gametogenesis. Nature 308, 548-50.

Tremblay, K. D., Saam, J. R., Ingram, R. S., Tilghman, S. M., Bartolomei, M. S., 1995. A paternal-specific methylation imprint marks the alleles of the mouse H19 gene. Nat. Genet. 9, 407-413.

Tsunoda, Y., Kato, Y., 2002. Recent progress and problems in animal cloning. Differentiation 69, 158-161.

Vestweber, D., Kemler, R., Ekblom, P., 1985. Cell-adhesion molecule uvomorulin during kidney development. Dev. Biol. 122, 213-221.

Wakayama, T., Perry, A. C. F., Zuccoti, M., Johnson, K. R., Yanagimachi, R., 1998. Full-term development of mice from enucleated oocytes injected with cumulus cell nuclei. Nature 394, 369-374.

Wakayama, T., Yanagimachi, R. 2001. Mouse cloning with nucleus donor cells of different age and type. Mol. Reprod. Dev. 58, 376-383.

Wang, Y., Joh, K., Mukai, T., 2002. Identification of a novel isoform of Murr1 transcript, U2mu, which is transcribed from the portions of two closely located but oppositely oriented genes. Genes. Genet. Syst. 77, 377-381.

Wang, Y., Joh, K., Masuko, S., Yatsuki, H., Soejima, H., Nabetani, A., Beechey, C. V., Okinami, S., Mukai, T., 2004. The mouse Murr1 gene is imprinted in the adult brain, presumably due to transcriptional interference by the antisense-oriented U2af1-rs1 gene. Mol. Cell Biol. 24, 270-279.

Whiteley, G. S., Fuller, B. J., Hobbs, K. E., 1992. Deterioration of cold-stored tissue specimens due to lipid peroxidation: modulation by antioxidants at high subzero temperatures. Cryobiology 29, 668-673.

Wilkie, AL., Jordan, S. A., Jackson, I. J., 2002. Neural crest progenitors of the melanocyte lineage: coat colour patterns revisited. Development 129, 3349-3357.

Wood, S.A., Allen, N. D., Rossant, J., Auerbach, A., Nagy, A., 1993. Non-injection methods for the production of embryonic stem cell-embryo chimaeras. Nature 365, 87-89.

Yamasaki, K., Joh, K., Ohta, T., Masuzaki, H., Ishimaru, T., Mukai, T., Niikawa, N., Ogawa, M., Wagstaff, J., Kishino, T., 2003. Neurons but not glial cells show reciprocal imprinting of sense and antisense transcripts of Ube3a. Hum. Mol. Genet. 12, 837-847.

Yamazaki, Y., Makino, H., Hamada-Hamaguchi, K., Hamada, S., Sugino, H., Kawase, E., Miyata, T., Ogawa, M., Yanagimachi, R., Yagi, T., 2001. Assessment of the developmental totipotency of neural cells in the cerebral cortex of mouse embryo by nuclear transfer. Proc. Natl. Acad. Sci. USA 98, 14022-14026.

Yang, A.H., Kaushal, D., Rehen, S. K., Kriedt, K., Kingsbury, M. A., McConnell, M. J., Chun., J., 2003. Chromosome segregation defects contribute to aneuploidy in normal neural progenitor cells. J. Neurosci. 23, 10454-10462.

Zambrowicz, B. P., Imamoto, A., Fiering, S., Herzenberg, L. A., Kerr, W. G., Soriano, P., 1997. Disruption of overlapping transcripts in the βgeo 26 gene trap strain leads to widespread expression of β-galactosidase in mouse embryos and hematopoietic cells. Proc. Natl. Acad. Sci. USA 94, 3789-3794.

Zuccotti, M., Monk, M., 1995. Methylation of the mouse Xist gene in sperm and eggs correlates with imprinted Xist expression and paternal X-inactivation. Nat. Genet. 9, 316-320.

Fig. 1. Strategy for generating DNnt aggregation chimeras.

Embryos at the 4- to 8-cell stage were cloned using the nuclei of neurons derived from the cerebral cortex of postnatal mice at P0 to P4 (DNnt embryos). Wild-type embryos were frozen and thawed at the 2-cell stage (Freeze&Thaw embryos). DNnt aggregates were made with a single DNnt embryo and a single Freeze&Thaw embryo. They developed into aggregated blastocysts 1 day after aggregation. Blue indicates DNnt cells that were derived from DNnt embryos. Green shows wild-type cells that were derived from Freeze&Thaw embryos. This strategy simultaneously generated DNnt and control chimeras.

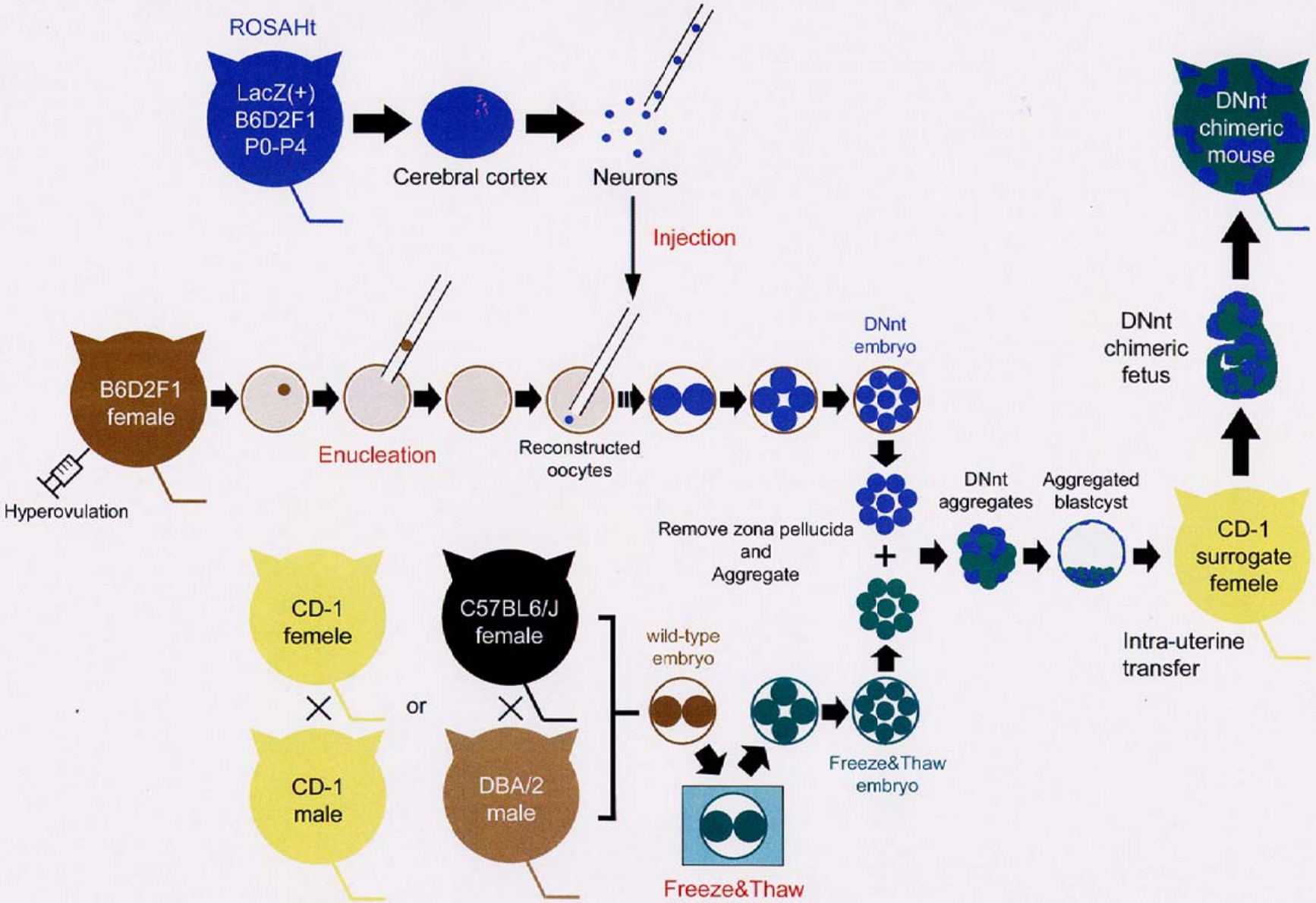
ROSAHt
LacZ(+)
B6D2F1
P0-P4
Cerebral cortex
Neurons
Injection
B6D2F1
female
Hyperovulation
Enucleation
Reconstructed
oocytes
DNnt
embryo
DNnt
chimeric
fetus
DNnt
chimeric
mouse
Remove zona pellucida
and
Aggregate
DNnt
aggregates
Aggregated
blastcyst
CD-1
surrogate
femele
Intra-uterine
transfer
CD-1
femele
or
C57BL6/J
female
CD-1
male
DBA/2
male
wild-type
embryo
Freeze&Thaw
embryo
Freeze&Thaw

Figure. 1

Fig. 2. Distribution of DNnt cells in the DNnt chimeric mouse.

The DNnt chimeric male mouse at P106 was made from a DNnt embryo carrying cloned nuclei of neurons derived from a P1 cerebral cortex and a Freeze&Thaw embryo (CD-1 x CD-1 F1). He had agouti hairs on his back that are indicated with an arrow (A and B).

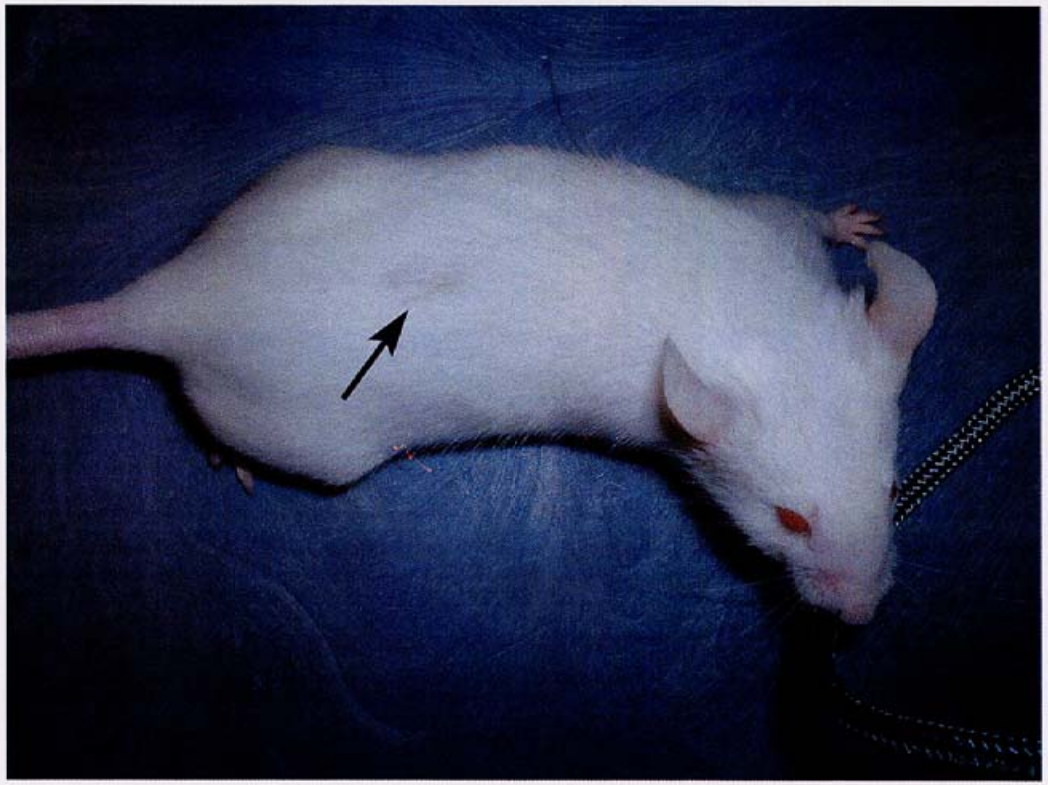

Figure. 2

Fig. 3. Distribution of DNnt cells in the DNnt chimeric pup.

The P1 female DNnt chimeric pup was made from a ROSAHt DNnt embryo carrying the cloned nuclei of neurons from a P3 cerebral cortex and a Freeze&Thaw embryo (B6 x DBA/2 F1). LacZ-positive cells were visible in the sagittally sectioned proximal renal tubules of her kidney (asterisks in B) and in her tail. LacZ-positive cells were not detected in the B6D2F1 specimens (asterisks in A). A ROSAHt B6D2F1 specimen contained LacZ-positive cells (asterisks in C). LacZ-positive cells are shown as sky blue or blue (B and C). Proximal renal tubules, glomeruli, and distal renal tubules are indicated with asterisks, "G," and arrows, respectively. Scale bars, 50 μm.

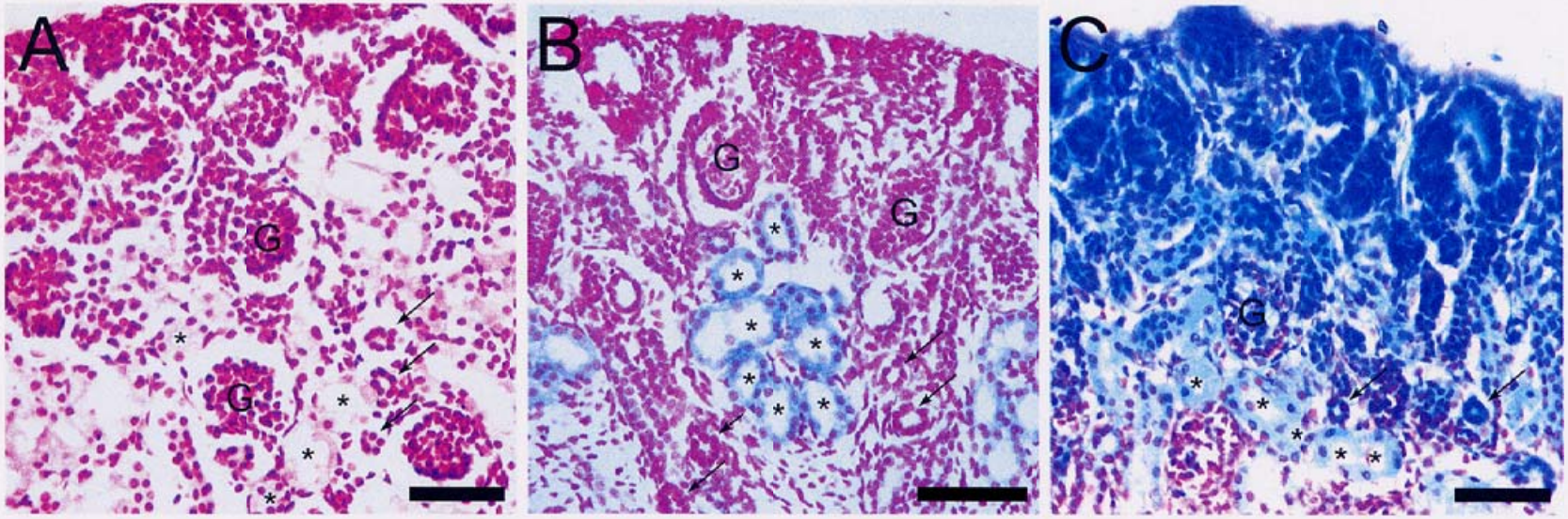

Figure. 3

Fig. 4. Distribution of LacZ-positive cells in the DNnt chimeric fetuses.

CH3 (A and D), CH4 (B and E), and CH5 (C and F) were produced from DNnt embryos and Freeze&Thaw embryos. Images show the left side (A, B, and C) and dorsal (D, E, and F) views of these chimeras. LacZ-positive cells were present both in the chimeric bodies and in the yolk sacs (arrow in A). CH5, which contained a large number of LacZ-positive cells, showed developmental retardation and a distended pericardial cavity (arrowhead in C). The locations of the LacZ-positive cells in these chimeric fetuses differed. Scale bars, 1 mm.

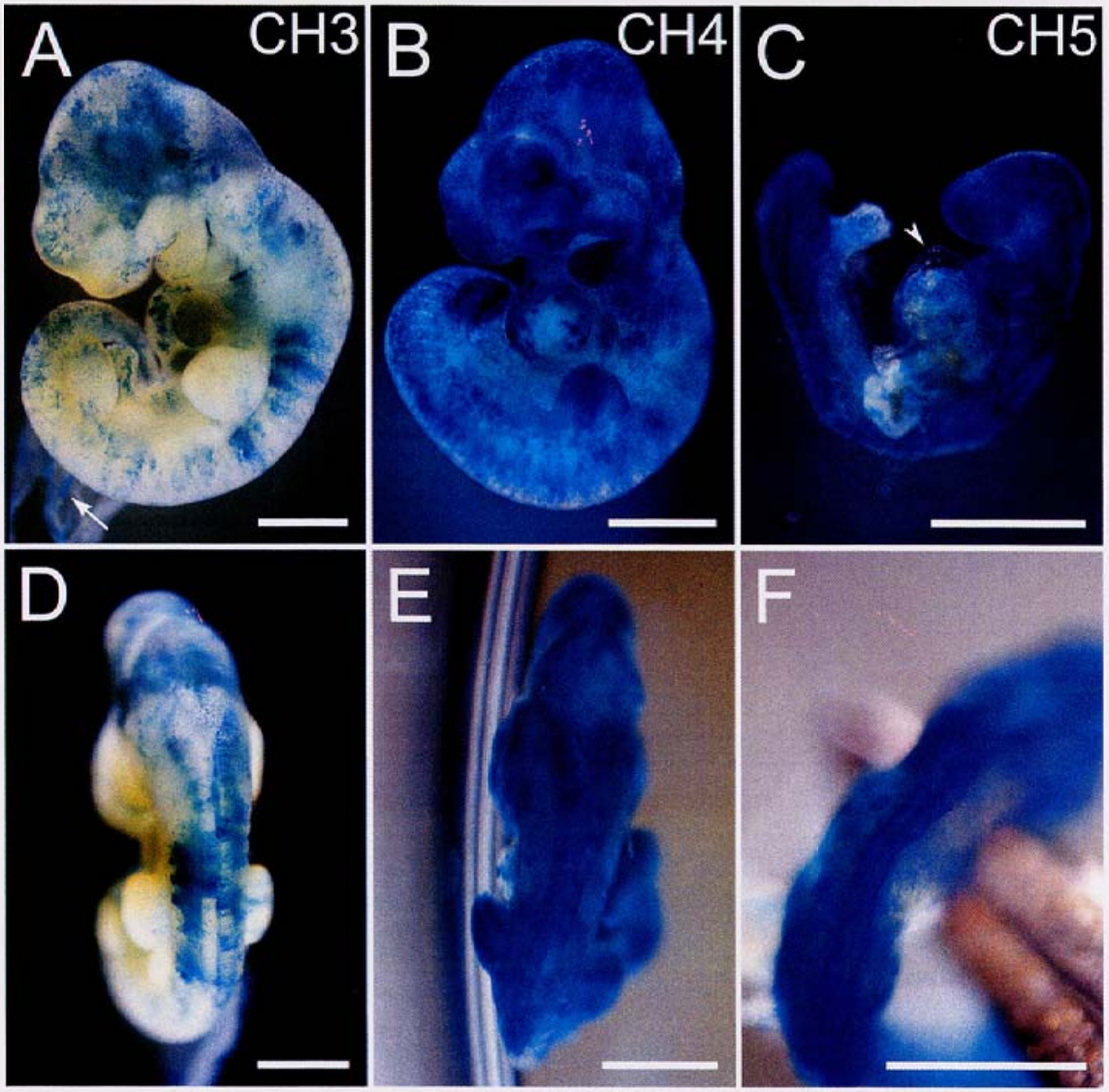

Figure. 4

Fig. 5. Localization of LacZ-positive cells in the neuroepithelium of the DNnt chimeric fetuses.

Sagittally sectioned neuroepithelium of the telencephalon in the control chimeric fetus (A and B) and CH3 (C and D) and CH4 (E and F) stained by Feulgen reaction after X-gal staining. The nuclei in the wild-type cells from Freeze&Thaw embryos are claret, and the LacZ-positive cells from the DNnt embryos are stained royal blue. The right panels show high-magnification images of the areas enclosed in the squares in the left side panels. Anterior to top, ventral to right. LacZ-positive cells were distributed widely (large arrows in B, D, and F). Wild-type cells are indicated by small arrows (F). LacZ-positive cells often lost their nuclei (arrowheads in D and F). More LacZ-positive cells were observed in CH4 than in CH3. CH4 showed frequent collapse of the ventricular surface of the neuroepithelium (double-headed arrows in E). Scale bars, 25 μm.

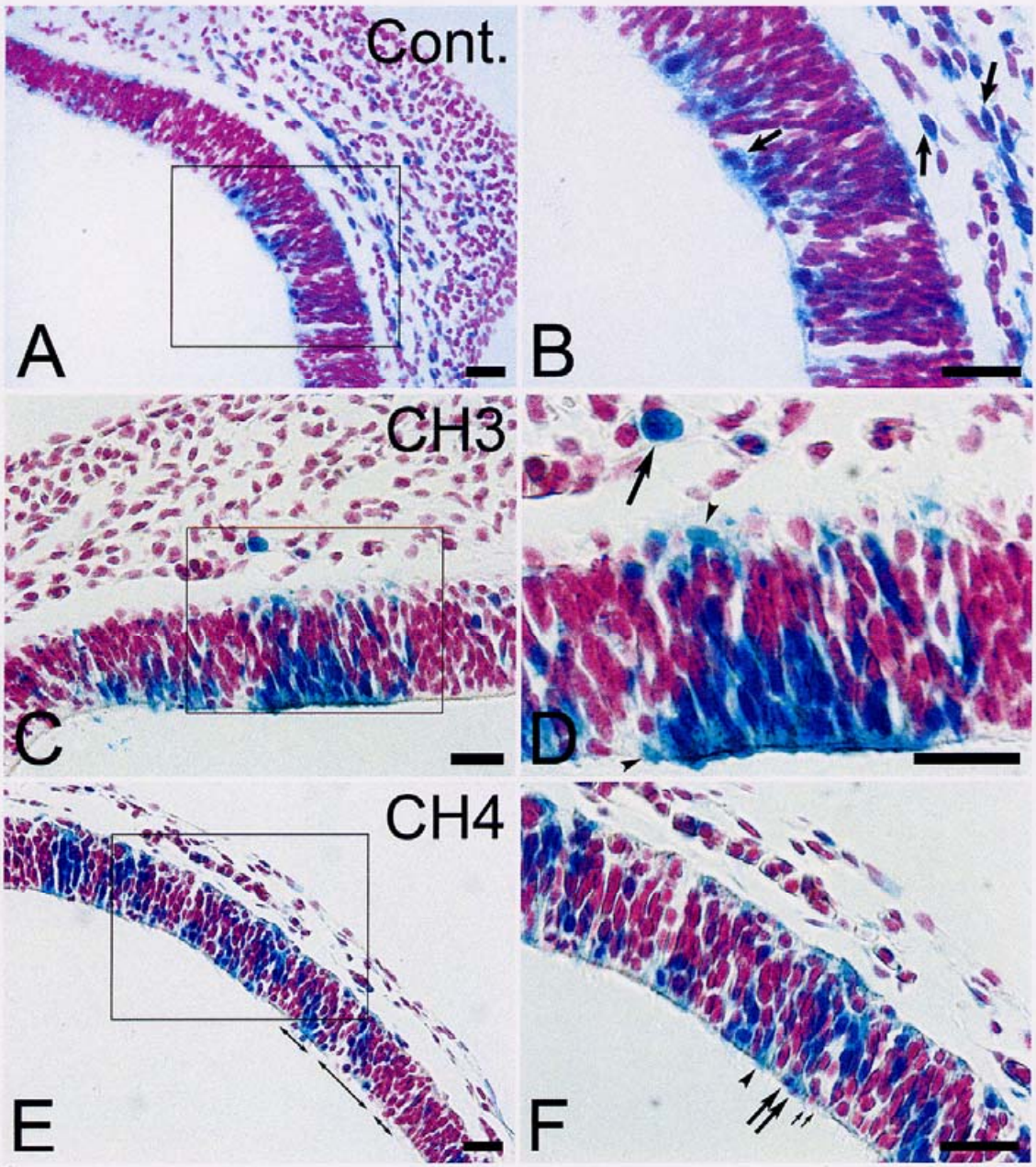

Figure. 5

Fig. 6. Contribution of LacZ-positive cells to the various tissues of the CH3 chimeric fetus, which had the smallest number of LacZ-positive cells of the three DNnt chimeric fetuses.

Sagittally sectioned neural tube near the tail (A and B), eye (C and D), heart (E and F), and forelimb bud (G and H) of CH3 stained by Feulgen reaction after X-gal staining. The nuclei of wild-type cells from Freeze&Thaw embryos are shown in claret, and the LacZ-positive cells from DNnt embryos are royal blue. The right panels show high-magnification images of the regions enclosed by the squares in the respective left panels. LacZ-positive cells contributed to tissues derived from the ectoderm, including the neural tube (A and B) and optic cup (C and D). They also contributed to tissues derived from the mesoderm, including the heart (E and F) and limb bud (G and H), and from the endoderm (Ma in E). Collapsed regions of the lumen of the neural tube were common (double-headed arrows in A). Lv, lens vesicle; In, inner (neural) layer of optic cup; Ou, outer layer of optic cup; Ma, mandibular component of first branchial arch; Ta, truncus arteriosus region; Ac, common atrial chamber of heart; A-Vc, wall of atrio-ventricular canal; Bc, bulbus cordis; H/Bp, hepatic/biliary primordial within septum transversum. Wild-type cells, LacZ-positive cells, and LacZ-positive cells without nuclei are indicated by small arrows (B, D, F, and H), large arrows (B, D, F, and H), and arrowheads (B), respectively. Scale bars in A, C, F and H, 50 μm. Scale bars in B and D, 25 μm; in E and G, 100 μm.

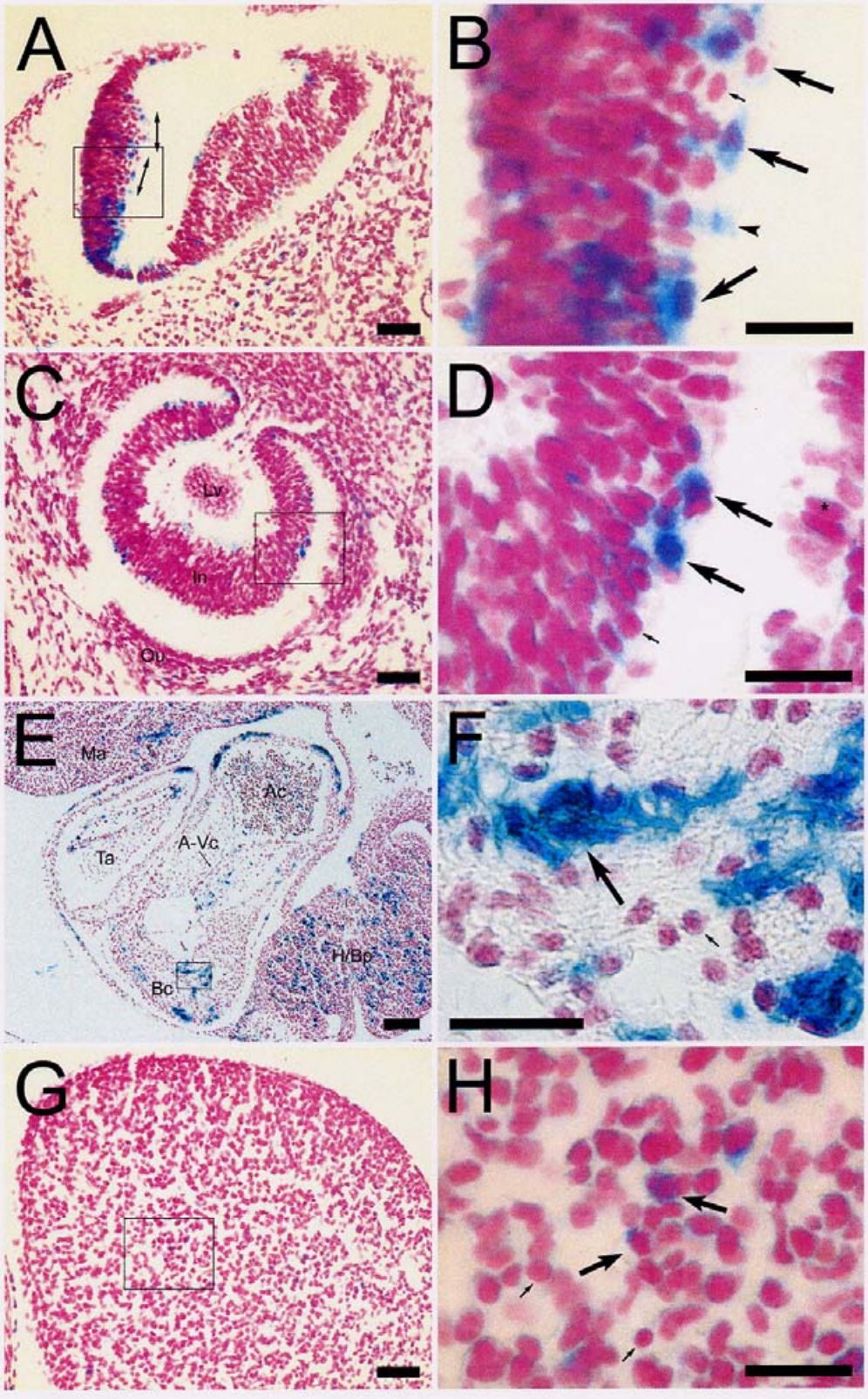

Figure. 6

Table 1
Effective conditions for generating aggregated blastocysts

Condition of wild-type embryos[§]	No. of DNnt aggregates	No. (%)[*] of aggregated blastocysts
Fresh	26	11 (42.3)
Freeze&Thaw	130	72 (55.4)

Note. [*]Percentage of aggregated blastocysts developed from DNnt aggregates. All DNnt and wild-type embryos were used at the 4- to 8- cell stage.

Table 2
Production of the DNnt chimeric pup and mouse

1) A chimeric mouse that was constructed from a DNnt and a Freeze&Thaw CD-1 embryo

No. of reconstructed oocytes	No. (%)* of oocytes activated	No. of DNnt aggregates	No. (%)§ of aggregated blastocysts	No. of embryos transferred	Total no. (%)* of mice	No. (%)* of mice with agouti hairs
469	380 (81.0)	54	37 (68.5)	54	27 (5.8)	1 (0.2)

2) A chimeric pup that was constructed from a DNnt embryo carrying the LacZ gene and a Freeze&Thaw B6D2F1 embryo

No. of reconstructed oocytes	No. (%)* of oocytes activated	No. of DNnt aggregates	No. (%)§ of aggregated blastocysts	No. of embryos transferred	Total no. (%)* of pups	No. (%)* of pups including LacZ positive cells
297	247 (83.2)	19	3 (15.8)	19	8 (2.7)	1 (0.3)

Note. *Percentage of oocytes, mice and pups that developed from reconstructed oocytes. §Percentage of aggregated blastocysts that developed from DNnt aggregates. All wild-type embryos were thawed after cryopreservation at the 2-cell stage.

Table 3
Generation of DNnt chimeric fetuses carrying the LacZ gene

No. of reconstructed oocytes	No. (%)* of oocytes activated	No. of DNnt aggregates	No. (%)§ of aggregated blastocysts	No. of embryos transferred	Total No. (%)* of fetuses	No. (%)* of chimeric fetuses	No. (%)* of chimeric fetuses	
							normal	abnormal
135	114 (84.4)	81	34 (42.0)	81	26 (19.3)	5 (3.7)	2 (1.5)	3 (2.2)

Note. *Percentage of oocytes and fetuses that developed from reconstructed oocytes. §Percentage of aggregated blastcysts that developed
from DNnt aggregates. *Percentage of embryos that developed from DNnt aggregates. All wild-type embryos were thawed after cryopreservation at the 2-cell stage.

Table 4
Morphological characteristics of DNnt chimeric fetuses

DNnt chimeric fetuses	Ages of donor cells	Heartbeat	Closed neural tube	Turning	Forelimb buds & hindlimb buds	Normal fetus	Chimerism with LacZ positive cells (%)*
CH1	P2	-	-	-	-	-	76-99
CH2	P3	-	-	-	-	-	76-99
CH3	P0	+	+	+	+	+	1-25
CH4	P0	+	+	+	+	+	76-99
CH5	P2	-	+	+	-	-	76-99

Note. *Percentage of chimerism based on the external X-gal staining.
+ denotes that the fetus met the standard indicated.

Table 5
Localization of LacZ-positive cells in the DNnt chimeric fetuses

DNnt chimeric fetuses	Ectoderm				Mesoderm				Endoderm	
	Lens	Neuroepithelium	Neural tube	DRG	Heart	Somite	Limb buds	Mesenchyme	Branchial arch	Hind gut
CH3	+	+	+	+	+	+	+	+	+	+
CH4	+	+	+	+	+	+	+	+	+	N.D.
CH5	+	+	+	+	+	+	+	+	N.D.	+

Note. + denotes tissues that contained LacZ-positive cells.

Acknowledgements

I would express my sincere appreciation to Profs. Takeshi Yagi (Osaka University), Ryuzo Yanagimachi (University of Hawaii, U.S.A.) and Kazuhiro Ikenaka (The Graduate University for Advanced Studies) for continuous encouragements and helpful advice throughout this study.

I thank Dr. Yukiko Yamazaki (University of Hawaii, U.S.A.) and Mr. Makoto Sanbo (National Institute for Physiological Sciences) for the technical instruction on the manipulation of mice embryos. I also thank Drs. Shun Hamada (Osaka University) and Kouji Senzaki (National Institute of Neuroscience) for the technical advice on the immunohistological analysis. I would express my gratitude to Profs. Ryuichi Shigemoto, Yasuo Kawaguchi (The Graduate University for Advanced Studies) and Dr. Tomoyuki Tokunaga (National Institute of Agrobiological Sciences) for the research advice.

I wish to thank all the members of the Division of Neurobiology and Behavioral Genetics in the National Institute for Physiological Sciences, the Institute for Biogenesis Research in the University of Hawaii and the KOKORO-Biology Group of the Graduate School of Frontier Biosciences in the Osaka University.

Finally, I apprecaite my parents and my friends from the bottom of my heart for supporting me in everything without compensation.

This research was supported by a grant from CREST (Core Research for Evolutional Science and Technology) of JST (Japan Science and Technology Corporation) (to Prof. Takeshi Yagi).